

2010

Catalytic oxidative desulfurization of a model diesel

Dongxing Liu

Louisiana State University and Agricultural and Mechanical College, liudongxing@gmail.com

Follow this and additional works at: https://digitalcommons.lsu.edu/gradschool_majorpapers



Part of the [Chemical Engineering Commons](#)

Recommended Citation

Liu, Dongxing, "Catalytic oxidative desulfurization of a model diesel" (2010). *LSU Major Papers*. 50.
https://digitalcommons.lsu.edu/gradschool_majorpapers/50

This Major Paper is brought to you for free and open access by the Graduate School at LSU Digital Commons. It has been accepted for inclusion in LSU Major Papers by an authorized graduate school editor of LSU Digital Commons. For more information, please contact gradetd@lsu.edu.

CATALYTIC OXIDATIVE DESULFURIZATION OF A MODEL DIESEL

A Thesis
Submitted to the Graduate Faculty of the
Louisiana State University and
Agricultural and Mechanical College
in partial fulfillment of the
requirements for the degree of
Master of Science in Chemical Engineering
in
The Gordon A. and Mary Cain Department of Chemical Engineering

by
Dongxing Liu
B.S., Tianjin Univeristy, China, 2007
August 2010

ACKNOWLEDGMENTS

I am deeply thankful to Dr. Knopf, for his great interest, encouragement and stimulating discussions throughout the progress of this work. I would like to thank Dr. Dooley for suggesting the topic, continuous guidance, great efforts and fruitful advice during the work. I would also like to thank Dr. Negulescu for pore size distribution measurement, and Dr. Dodla for the ICP-AES measurements in the Central Analytical Instruments Research Laboratory at LSU. I wish also to extend my thanks to the workshop of the Department of Chemical Engineering. Also, I wish to express my deep thanks to NSF for supporting this work. Finally, I wish to thanks my friends Yijie Shen, Rong Bai, Qiang Sheng, for standing beside me during this work and encouraging me.

I also thank my family, my parents, my brother and sister.

TABLE OF CONTENTS

ACKNOWLEDGMENTS	ii
ABSTRACT	iv
CHAPTER 1 INTRODUCTION AND LITERATURE REVIEW	1
1.1 THE NEED FOR LOW SULFUR FUEL	1
1.2 THE RATIONALE FOR OXIDATIVE DESULFURIZATION (ODS).....	2
1.3 CURRENT HYDRODESULFURIZATION PROCESS.....	3
1.4 ODS WITH OXYGEN	4
1.5 ODS WITH OXYGEN AND ALDEHYDE.....	5
1.6 ODS WITH ADDED PEROXIDE	7
1.7 ODS WITH OIL-SOLUBLE PEROXIDES	11
1.8 ODS WITH SOLID OXIDANTS:	13
1.9 THE GOAL OF THIS RESEARCH WORK.....	13
CHAPTER 2 EXPERIMENTAL METHODS	15
2.1 CATALYST PREPARATION.....	15
2.2 SEMIBATCH REACTOR EXPERIMENTS.....	18
2.3 ANALYSIS OF PRODUCT SAMPLES	19
2.4 CATALYST CHARACTERIZATION	20
2.5 COATING OF MONOLITHS FOR FUTURE WORK	20
CHAPTER 3 RESULTS AND DISCUSSION.....	23
3.1 CATALYST CHARACTERIZATION RESULTS	23
3.2 ANALYSIS OF OXIDATION PRODUCTS.....	26
3.3 ACTIVITY AND SELECTIVITY OF THE CATALYSTS.....	30
CHAPTER 4 SUMMARY AND CONCLUSION	42
REFERENCES	46
APPENDIX A GC PARAMETER	53
APPENDIX B PROCEDURE TO PERFORM THE EXPERIMENT	56
APPENDIX C RAW DATA AND REACTION CONDITIONS	58
APPENDIX D CATALYST CHARACTERIZATION.....	66
VITA.....	72

ABSTRACT

An analysis of heterogeneous oxidation catalysts was performed to determine the activities and optimal operating conditions for the multiphase oxidative desulfurization (ODS) reactions, using a model diesel. Catalysts studied included well-characterized Pd on Al_2O_3 and activated carbon supports, and carbon-supported Mo_2C and W_2C , which were prepared by temperature programmed reaction. Several other typical oxidation catalysts were also examined.

The model diesel consisted of ~1 wt% sulfur compounds (thiophene and dibenzothiophene) with appropriate amounts of aliphatic, alkylaromatic and N-heterocyclic compounds to simulate a raw number 2 diesel. With oxygen as the oxidant in ODS reactions of this model diesel (70-90°C, 0.8-1.8 MPa, feed vol/wt cat. = 100 mL/g), Pd/C and $\text{Mo}_2\text{C}/\text{C}$ showed the best selectivity for oxidizing the N- and S-heterocycles vs. the alkylaromatics. Increasing the pressure increased the reaction rates of the N- and S-heterocycles. Except for thiophene, there was only a small dependence of observed rates on temperature, which suggests the reactions were partially diffusion (of O_2) controlled. The optimal ODS catalysts (carbides and 5%Pd/MPT-5) also showed high activity for the conversion of N-heterocycles.

Current work includes further investigations of the better catalysts, full characterization of the products by GC-MS, and kinetics measurements using catalyst monoliths in a piston-oscillating reactor, which can eliminate the diffusion limitations and provide a uniform hydrodynamic environment.

CHAPTER 1 INTRODUCTION AND LITERATURE REVIEW

1.1 The Need for Low Sulfur Fuel

There is an increasingly stricter trend in the legislative regulations on sulfur content in transportation fuels in most western countries for past two decades. For example, the U.S. Environmental Protection Agency has limited the sulfur content of most diesel fuels to 15 ppm from a level of 500 ppm in 2006.¹ The environmental regulations for on-road diesel fuels in Europe called for sulfur content reductions from the level of 350 to 50 ppm by 2005 and to 10 ppm by 2009.² Similarly, Japan imposed a decrease from 500 to 50 ppm by the end of 2004 and is planning to further lower this limit down to 15 ppm. All of this takes place at a time when the average amounts of sulfur in crude oils are increasing.

Because of their availability, low cost, ease of storage and high energy density, liquid hydrocarbon fuels such as gasoline, jet fuel and diesel are also considered to be potential fuels for fuel cells, for example in portable power applications. The hydrocarbon fuels are catalytically reformed to a hydrogen-rich gas that can react catalytically with oxygen in the fuel cell stack for electricity generation. However, even trace amounts of sulfur (a few ppm by weight) can poison both the fuel processing and the electro-catalyst in the fuel cell.² The H_2S , S or SO_x can also poison catalysts for the conversion of NO_x , CO, and particulate matter in the exhaust gas catalytic converters of vehicles. In summary, the petroleum refining industry faces major challenges in economically producing ultra-clean liquid hydrocarbon fuels to meet new and stricter sulfur specifications and to meet the needs of fuel cell applications.

In a petroleum refinery, the desulfurization and denitrogenation of petroleum feedstocks is important for three reasons.³ First, high levels of sulfur-containing organics in the feed can contaminate supported platinum reforming catalysts during the catalytic reforming stage. Second, the removal of sulfur-containing compounds from feeds can improve the color and

stability of products such as gasoline from catalytic cracking units (referred to as a sweetening process). Third, removal of organic nitrogen compounds from the feed to catalytic cracking units can avoid the neutralization of the acidic catalyst by the basic nitrogen compounds.

1.2 The Rationale for Oxidative Desulfurization (ODS)

Achieving lower sulfur contents in fuels with current hydrodesulfurization (HDS) technology requires the use of a higher reaction temperature, a higher reaction pressure, a larger reactor volume, or more active catalysts, or some combination of these.⁴ All of these cost money. There are also some inherent problems for HDS in converting heterocyclic sulfur-containing compounds such as it's the methylated derivatives of DBT, such as 4-methyldibenzothiophene and 4,6-dimethyldibenzothiophene (4,6-DMDBT). These compounds are sterically hindered in dehydrogenation,⁵ and also their C-S bond energy is almost equal to the C-H bond energy, which makes them hard to desulfurize by hydrotreatment.⁶

Therefore, several new processes as alternatives to HDS have been proposed, for example selective sulfur adsorption, selective sulfur oxidation and biodesulfurization.⁴ Above among these, oxidative desulfurization (ODS) appears promising, because it has some potential advantages over HDS. First, it does not require hydrogen, and, second, the process can be conducted at relatively mild conditions (usually 313-373 K and 0.1-0.2 MPa).⁷ The oxidation of sulfur containing compounds in the fuels leads to the formation of the corresponding sulfoxides / sulfones, which are highly polar and can be separated by extraction with polar solvents (acetonitrile, methanol, *N,N*-dimethylformamide, etc.).⁷ Third, the most refractory aromatic sulfur containing molecules such as the derivatives of DBT are more easily converted to their sulfones than is thiophene.¹⁷ Several studies on both oxidants and catalysts have been published (see below) and some catalysts show significant activity

for the oxidation of DBT, benzothiophene (BT), and other sulfur-containing organic compounds. Based on the oxidant, ODS systems can be broadly classified as either oxygen-based ODS, or peroxide-based ODS.

1.3 Current Hydrodesulfurization Process

The current HDS that is widely employed in the petroleum refining not only forms H_2S by reacting the sulfur in sulfur-containing organic compounds (e.g., mercaptans, disulfides, thiophenes, benzothiophenes and dibenzothiophenes), but also forms NH_3 by reacting organic nitrogen compounds (e.g., aliphatic amines, pyrroles, pyridines, acridines, carbazoles) with high pressure hydrogen.

Catalysts are usually either an alumina-supported mixture of cobalt and molybdenum oxides or nickel and tungsten oxides. In the reactor environment these partially reduced oxides are converted to their sulfide forms. Indeed, before refinery streams are fed to a hydrotreating unit, the catalyst is deliberately sulfided. The H_2S product is then in sufficient quantity to keep the catalyst sulfided and prevent reduction of the catalyst to the inactive metal. Some authors have proposed a monolayer of S^{2-} ions superimposed over a second layer containing O^{2-} , Mo^{3+} and Mo^{5+} , and stabilized by Co promoter ions contained in sublayers of the underlying support.⁸ Other authors have suggested that intercalation of cobalt or nickel occurs at the edges of partially reduced structures of MoS_2 or WS_2 .⁸

HDS takes place at 593-653 K and 3-7 MPa over sulfided CoMo or NiMo catalysts. The major sulfur compounds existing in current liquid hydrocarbon fuels are thiophenic compounds and their alkyl-substituted derivatives. The alkyl-substituted derivatives are considered to be the most refractory sulfur compounds in the fuels due to the steric hindrance of the alkyl groups in HDS.⁴ Typical HDS catalysts are Co (or Ni)-promoted Mo/Al_2O_3 .⁹

1.4 ODS with Oxygen

This type of ODS employs oxygen in air to oxidize the sulfur compounds. Few publications fall into this category. Sampanthar et al. 2006 reported that $\text{MnO}_2/\text{Al}_2\text{O}_3$ and $\text{Co}_3\text{O}_4/\text{Al}_2\text{O}_3$ can catalyze the air oxidation of the refractory sulfur impurities in real diesel to their corresponding sulfones at 403-473 K and 0.1 MPa air.¹⁰ The sulfur content was reduced to 40-60 from 400 ppm in the feed after extraction by 1-methyl-2-pyrrolidinone (NMP). However, after oxidation the olefin content of the diesel increased from 2.4 % to 3.6 %, the aromatic content of the diesel decreased from 46.4% to 12.5%, and the cetane index increased by 20%, all of which are consistent with the oxidation of the aromatics in the treated diesel. The authors also found some SO_2 , which was confirmed by scrubbing the outlet gas with a AgNO_3 solution to form AgSO_3 precipitate. They also found that oxidation was not observed below 383 K, and that for the case of $\text{MnO}_2/\text{Al}_2\text{O}_3$ a higher Mn loading led to higher conversion at all reaction temperatures. However, for $\text{Co}_3\text{O}_4/\text{Al}_2\text{O}_3$, differences in Co-loading did not lead to significant differences in conversion. The reactivity of sulfur compounds in this system was: 4, 6-DEDBT > 4, 6-DMDBT > 4-MDBT > DBT, where M = methyl, E = ethyl, D = di-.

It was reported that $\text{CuO}/\text{ZnO}/\text{Al}_2\text{O}_3$ (atomic ratio of 57/20/66 Cu/Zn/Al), 1.5% Pt/CeO₂ and Cu/CeO₂ (atomic ratio of 1/4 Cu/Ce) catalyzed the conversion of sulfur compounds (thiophene, DBT, BT, 1-pentanethiol, and dibutyl sulfide) in isooctane to SO_2 at 573 K, 0.1 MPa.¹¹ This temperature was needed to maintain the activity of the catalyst because only here could the SO_2 desorb. At a lower temperature (523 K), the accumulation of sulfite on the catalyst surface caused deactivation, which was confirmed by diffuse reflectance infrared Fourier transform spectroscopy, peaks at 1220 and 990 cm^{-1} . The activity of the catalyst toward different sulfur- containing compounds at 573 K (95% conversion) were: thiophene, at O/S molar ratio = 110 and WHSV = 7 h^{-1} ; DBT, at O/S = 95 and WHSV

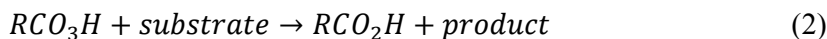
= 13 h⁻¹; 1-pentanethiol and dibutyl sulfide, O/S = 10~15 and WHSV = 30 h⁻¹. The authors also found (by DRIFTS) that the adsorption of thiophene can take place even at room temperature, and more easily than paraffinic, olefinic, and aromatic hydrocarbons.

Song et al.⁷ studied ODS of liquid hydrocarbon fuels (model jet fuel, 0.047 wt% of BT, 0.0675 2-MBT, 0.048 5-MBT, 0.0595 DBT, 0.0398 naphthalene, 0.0477 2-methylnaphthalene, 9.996 tert-butybenzene, 44.33 n-decane, 0.0592 n-hexadecane and 44.33 wt% of n-tetradecane, and JP-8, total sulfur 717 ppmw) was catalyzed by Fe(III) salts (nitrate/bromide, wt ratio 1/3, denoted Fe-Fe) supported on activated carbon (AC). At 0.1 MPa and 298 K, 38% of the DBTs and BTs were oxidized to the corresponding sulfones in 5 h with fuel/adsorbent ratio of 21. The adsorption on activated carbon of thiophenic compounds in the model jet fuel and oxidized fuel was also investigated. They found that the activated carbon had a higher adsorption selectivity for DBTs and sulfones than for BTs. The reactivity of the sulfur compounds for oxidation over Fe(III) catalyst increased in the order: DBT < BT < 5-MBT < 2-MBT. The authors explained that “the methyl group on BT increases the oxidation reactivity, probably because the methyl group on the aromatic rings is an electron donor, which enhances the electron density of the sulfur atom....” Therefore they are assuming that the active oxygen is electrophilic (e.g., a peroxy radical or superoxide). They also found that increased loading (33%) of Fe(III) salt further the oxidation activity, so Fe is involved in forming the active site.

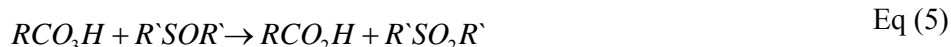
1.5 ODS with Oxygen and Aldehyde

Most previous work in ODS has focused on peroxide oxidants. Although ODS with peroxides is attractive because the reaction conditions are mild, the large scale of use and storage of peroxides is dangerous and costly. Therefore there has been some work to generate the peroxide species in-situ. It was reported a homogenous system using O₂ and an aldehyde (octanal), with a cobalt salt as catalyst.¹² According to them, the ODS reaction can be divided

into two steps: first, the oxidation of the aldehyde with molecular oxygen to the corresponding peroxyacid, and, second, the oxidation of DBT with the peroxy acids.



A chain-radical mechanism was proposed, where the aldehyde is first oxidized by the metal salt to give a proton and an acyl radical (eq. 1). The acyl radical adds O₂ easily, to form the acylperoxy radical (eq. 2), which reacts with an aldehyde to give a peracid and regenerate the acyl radical (eq. 3). Then the peroxyacid oxidizes the sulfur heterocycle twice to give a sulfone (eq. 4-5).



Different oxidants affected the oxidation of DBT. With a relatively small oxidant such as performic acid (prepared from formic acid and hydrogen peroxide), DMDBT reacted more rapidly than DBT because the electron density of the sulfur atoms in DMDBT is higher.¹³ In contrast, DBT reacted more rapidly than DMDBT by using a hydrogen peroxide-polyoxometalate system, which is more sterically constrained but which could also generate a different active oxidant.¹⁴

There is a report of a heterogenous catalyst-oxygen-aldehyde system using Co and Mn oxides.¹⁵ Here, leached Co may also play a role as a homogeneous catalyst.

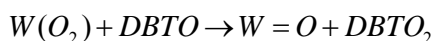
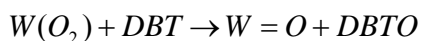
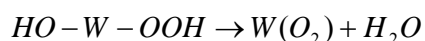
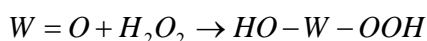
1.6 ODS with Added Peroxide

While there have been reports of ODS using aqueous H_2O_2 as oxidant, the insolubility of aqueous H_2O_2 in hydrocarbons is an obstacle; the reaction could only take place at the interface.¹⁶ Using a solvent to extract organosulfur compounds into the aqueous phase is one way to overcome the solubility limitation. These solvent (often acetonitrile)/substrate biphasic systems employ various catalysts, such as the typical nucleophilic oxidation catalysts (more often used with oxygen at higher temperatures) $\text{V}_2\text{O}_5/\text{TiO}_2$ and $\text{V}_2\text{O}_5/\text{Al}_2\text{O}_3$.^{17,18} In a synthetic diesel (composition: 847 ppmw of 2-methylthiophene (2-MT), 720 2,5-dimethylthiophene (2,5-DMT), 612 benzothiophene (BT), 445 dibenzothiophene (DBT), 414 4-dimethyldibenzothiophene (4-MDBT) and 387 4,6-dimethyldibenzothiophene (4,6-DMDBT), dissolved in hexadecane), the conversion of DBT catalyzed by $\text{V}_2\text{O}_5/\text{TiO}_2$ was ~80% at 333 K and with an oxygen to sulfur ratio of 2.13. Acetic acid was used to dissolve Na_2WO_4 , which also catalyzes ODS of DBT to its sulfone with H_2O_2 . By combining ODS and methanol extraction, the sulfur level in a hydrotreated diesel was reduced from 1100 to 40 ppm.¹⁹ It was reported that DMDBT in model fuel can be selectively oxidized by H_2O_2 ($\text{H}_2\text{O}_2/\text{S} < 4$) over Ti-WMS (Ti-containing wormhole mesoporous silica) and Ti-HMS (hexagonal mesoporous silica, similar to MCM-41).²⁰ It was investigated the catalytic activity of three different types of vanadosilica molecular sieves (MFI, MEL and HMS structures) in the oxidation of BT and DBT in a commercial light oil (425 ppm sulfur, 74.9 ppm nitrogen, 78.4 vol% saturated fraction and 21.6 vol% aromatics) with H_2O_2 at 333 K and a molar ratio of H_2O_2 / sulfur of 1000.²¹ The V-HMS showed the highest activity and also denitrogenated the light oil; pore diffusion may have been a factor here, because the V-HMS has mesopores. Another example of using mesopores to overcome the slow diffusion rates of the large sulfur heterocycles is to prepare mesoporous titanium silicate-1 (TS-1),²² synthesized using a CMK-3 carbon as template. It was used as an ODS catalyst at 333 K. The activity of the

mesoporous TS-1 was greater than that of TS-1. DBT was also oxidized with 12-tungstophosphoric acid (TPA) in the *n*-octane/acetonitrile biphasic system to give the corresponding sulfones as the major products.²³

Solid bases (hydrotalcites and La₂O₃) have also been used as ODS catalysts with H₂O₂.^{14,15,24} Another research used a W-containing hydrotalcite at 323 K to oxidize thiophene derivatives at a H₂O₂ to sulfur ratio of 5.²⁵ Other bases such as H₂O₂/Na₂CO₃ can remove 90% of 4,6-DMDBT (dimethyl-dibenzothiophene) at 323 K and a peroxide/S ratio of 32000.²⁶ In this paper, it was claimed that “H₂O₂ is the principal oxidizing agent; however, in the presence of Na₂CO₃ carbonate radicals (CO²⁻₃) are formed which could help catalyze...”

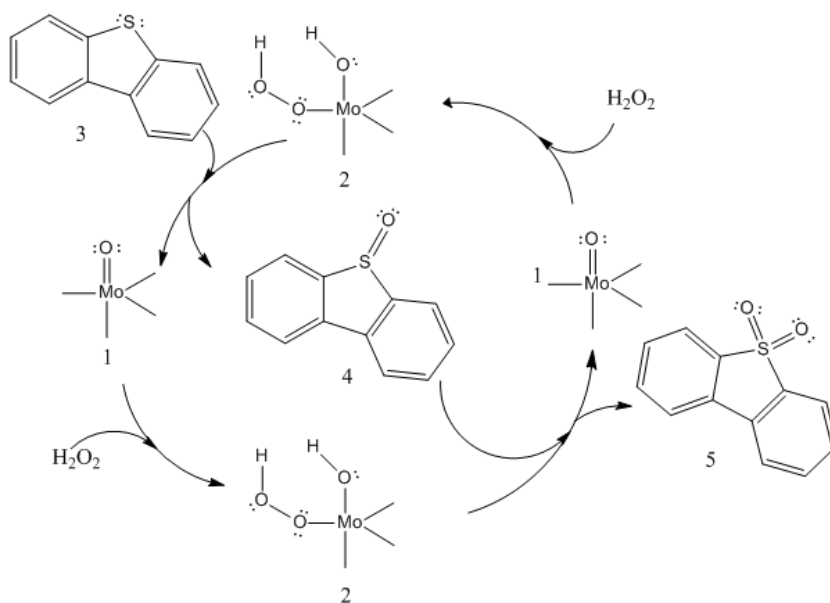
Catalysts normally considered to be strong or moderately strong Lewis and/or Bronsted acids have also been used. For example, oxidation can be carried out with WO_x-ZrO₂.²⁷ The authors claimed that Lewis acid sites on the catalyst surface dramatically enhance the electrophilicity of H₂O₂ toward the reaction with the weak nucleophile DBT. They postulated a surface peroxo-tungsten intermediate (W-O-O-H) for DBT oxidation. There was some Raman evidence for the interaction of a surface W = O with H₂O₂ and DBT. The proposed elementary reactions were:



where W(O₂) is a peroxo species.

One author experimented with ODS of several model S-heterocycles and of Mexican diesel using Mo/Al₂O₃ with H₂O₂ / acetonitrile.²⁸ They proposed a mechanism in accord with other peroxide-based oxidations in the literature (Scheme 1). A hydroperoxymolybdate species (2) is formed by the nucleophilic attack of H₂O₂ on Mo(VI) hepta- and

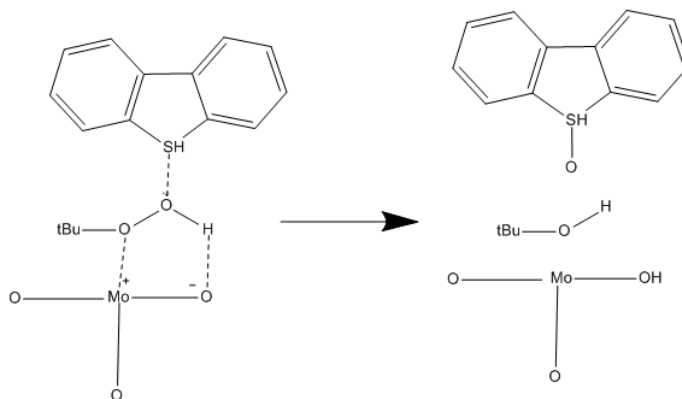
octamolybdates (1). Electron withdrawal from the peroxy ligand increases its electrophilic character. The oxidation of the sulfur atom (3) proceeds by nucleophilic attack of (2) to form the sulfoxide (4) and a regenerated Mo(VI) species (1). Subsequently, the sulfoxide (4) undergoes further oxidation by the hydroperoxymolybdate (2) to form sulfone (5). The presence of electronegative species adsorbed on the support (e.g., phosphates) promotes the reaction by withdrawing electron density from the peroxymolybdates.



Scheme 1 The proposed mechanism for oxidation of DBT using Mo/Al₂O₃ with H₂O₂ / acetonitrile²⁸

It was proposed a model for the initial stage of the hydroperoxide - MoO₃ complex.²⁹ From crystal structure analysis, the distance between Mo and oxygen atoms in MoO₃/Al₂O₃ is 1.96 Å, which is close to the O-H distance of a proposed peroxy-Mo(VI) complex (Scheme 2).³⁰ This suggests that the coordination of the hydroperoxide to Mo-O is promoted by the polarization of Mo^{d+} - O^{d-}; the pseudo-cyclic peroxide then reacts with the sulfur heterocycle. They found that the activation energy was almost the same for the ODS series of BT, DBT, 4-MDBT, 4,6-DMDBT in kerosene, at ~28.1 kJ/mol, suggesting all follow the same

mechanism.³⁰ Similarly, they did not find any significant difference in the ODS activation energy of DBT, 4,6-DMDBT and C3-DBT in a light oil, with a value of ~32.1 kJ/mol. The 4 kJ/mol difference was attributed to a solvent effect. For kerosene feed, the optimal O/S ratio was close to stoichiometric (~3), while in the case of the light gas oil it was ~15, suggesting a lower selectivity, so competitive reactions could also be responsible for an increase in the observed activation energy.



Scheme 2 Proposed peroxidic oxidation mechanism of DBT by t-BuOOH on MoO₃ catalyst³⁰

Even certain ACs can catalyze biphasic ODS of DBT with H₂O₂.³¹ The authors suggest that ACs have three roles in the reaction. First, selective adsorption on AC increases the collision probability of DBT and the peroxide. Second, hydroxyl radicals produced from H₂O₂ can be resonance-stabilized on the carbon surfaces. Third, a hydrophobic AC has a strong affinity for the oil phase, so activated carbon has a phase-transfer function.

There have been a few reports of noble metal-catalyzed ODS. It was reported that Au-, Ag-, or Pt-modified TiMWW (a Ti-containing zeolite) shows a much higher activity than that of TiMWW.³² Other researcher used Pd/MgO-Al₂O₃, Pd/Al₂O₃ and Pd/ZrO₂ to catalyze the oxidation of thiophene, BT and DBT in hexadecane at 333 K.³³ The Pd catalysts (1 wt.%) were prepared by impregnating the supports with aqueous PdCl₂·2H₂O, drying at 383 K, and then calcining at 673 K. Before testing, all the catalysts were reduced in H₂ at 773 K, which

normally gives low dispersions. For 165/1 (molar) $\text{H}_2\text{O}_2/\text{S}$, the 1% Pd/MgO- Al_2O_3 catalyst gave conversions of 85, 81 and 78% for thiophene, BT and DBT, respectively, in 50 min.

Another way to overcome the diffusion limitations associated with oil – aqueous H_2O_2 biphasic systems is to use amphiphilic phase transfer catalysts. The most common of these for ODS are the quaternary ammonium heteropolyoxotungstates. However, they are normally not very active. An exception was the work of Luo et al,³⁴ who studied the ODS of DBT in n-octane using a mixture of H_2O_2 , octadecyltrimethylammonium bromide (STAB), and phosphotungstic acid without pretreatment. After 10 min at 343 K with excess H_2O_2 ($\text{H}_2\text{O}_2/\text{DBT} = 18/1$ molar), almost 98 % of DBT reacted.

1.7 ODS with Oil-Soluble Peroxides

All of the above processes were limited to batch reactors, primarily because of the difficulties in mixing the aqueous and organic liquid phases. But a flow-type process would allow one to process large amounts of fuel, and a hydrocarbon-soluble peroxide such as tert-butyl hydroperoxide (TBHP) is suitable. Many catalysts have been found to be effective with a TBHP oxidant. Angelici reported the silica-catalyzed oxidation of DBT and 4,6-DMDBT by TBHP at 323-363 K with a 10/1 molar ratio of TBHP to DBT . The sulfur concentration in a simulated hydrotreated fuel (45 vol% toluene/ 55 vol% hexane) was reduced from 374 to 1 ppm in 40 min at 363 K.³⁵ Others investigated the effects of support on the catalytic activity of $\text{MoO}_3/\text{silica-alumina}$ (1% silica) and Bi-promoted $\text{MoO}_3/\text{silica-alumina}$.³⁶ One researcher studied the TBHP- assisted ODS of DBT in a fixed bed reactor catalyzed by Ti-MCM41, which was more active than $\text{MoO}_3/\text{Al}_2\text{O}_3$; Ti did not leach from the support.³⁷ Another study tested two supported heteropolyacids ($\text{H}_3\text{PMo}_{10}\text{V}_2\text{O}_{40}$ and $\text{H}_3\text{PMo}_{12}\text{O}_{40} / \text{Al}_2\text{O}_3$) for the ODS of pre-hydrotreated diesel using TBHP.³⁸ The $\text{H}_3\text{PMo}_{10}\text{V}_2\text{O}_{40}/\text{Al}_2\text{O}_3$ was more active, while $\text{H}_3\text{PMo}_{12}\text{O}_{40}/\text{Al}_2\text{O}_3$ was more selective, with lower TBHP consumption per turnover. The oxidation of DBT in a model diesel (45 vol% toluene/55 vol% hexane) was also achieved

using an immobilized oxorhenium(V) dithiolate ($\text{SiO}_2\text{-RTA})\text{Re}(\text{O})(\text{Me})(\text{PPh}_3)$ that oxidizes 9.45 mM DBT at 323 K with a 3/1 molar ratio of TBHP to DBT.³⁹

Ishihara et. al. found that *t*-BuOOH could oxidize the sulfur compounds in kerosene at ~ 353 K, an TBHP/S molar ratio of 3, and a WHSV of 60 h^{-1} , in the presence of a 16 wt.% $\text{MoO}_3/\text{Al}_2\text{O}_3$.⁴⁰ The mechanism to form the sulfone was proposed as sequential with one TBHP reacting with DBT first to the sulfoxide, then to the sulfone. The active intermediate would be a metal peroxide formed by the reaction of an oxometal group with TBHP.⁴¹ All of these observations can be explained by the oxidation mechanisms of Overberger and Cummins,⁴² and Bateman and Hargrave.⁴³ They postulated that the sulfur was oxidized by a nucleophilic attack on a peroxidic complex containing both peroxidic and protic structures.

Kabe et al. tested a series of catalysts supported on Al_2O_3 and found that the catalytic activity decreased in the order $\text{MoO}_3 > \text{WO}_3 > \text{V}_2\text{O}_5 > \text{Nb}_2\text{O}_5 > \text{ZrO}_2 > \text{CrO}_3$, for ODS of DBT with TBHP.³⁰ The details of the proposed mechanism are similar to those of Ishihara et al.⁴⁰ discussed above (Scheme 2), with TBHP being transformed to *t*-butanol. As no sulfoxide was detected under any reaction conditions, the rate-determining step was assumed to be sulfide \rightarrow sulfoxide. Interestingly, the introduction of Co and Ni into $\text{MoO}_3/\text{Al}_2\text{O}_3$ led to a remarkable decrease in activity, in contrast to HDS.

Regarding the surface structure of a $\text{MoO}_3/\text{Al}_2\text{O}_3$ catalyst, it is commonly accepted that Mo interacts with hydroxyl groups at coordinatively unsaturated Al^{3+} sites, and this interaction results in the polarization of Mo–O bond. For Co-promoted $\text{MoO}_3/\text{Al}_2\text{O}_3$, however, the Co ions occupy octahedral sites just below the Al_2O_3 surface, or tetrahedral sites in the bulk Al_2O_3 . It can therefore be inferred that occupation of these sites by Co or Ni did not enhance the polarization of the Mo–O bond. MoO_3 supported on $\text{SiO}_2\text{-Al}_2\text{O}_3$ or TiO_2 also showed lower oxidation activity, and while this could have been a result of greater TBHP decomposition on these supports, they contended that it resulted from fewer coordinatively

unsaturated Mo sites on these supports compared to Al_2O_3 . The oxidation activity for DBT increased with increasing Mo up to about 16 wt%, which may have corresponded to monolayer dispersion. The decrease in the activity at higher Mo content was attributed to fewer $\text{Mo-O-Al}^{3+}\text{-OH}$ sites.

1.8 ODS with Solid Oxidants:

The above ODS process based on a liquid phase oxidant shows promise for high desulfurization efficiency on an oil refinery stream. However, its industrial applicability would still be difficult or expensive, because of the widespread use of two liquid phases for the reactant mixture, which then requires a liquid-liquid separation step to remove both the spent oxidants (TBHP and aqueous H_2O_2 solution) and the oxidized products from the treated stream. Therefore, the use of solid catalysts and either solid or gaseous oxidizing agents in ODS processes is highly desirable, with evident advantages for the separation of the oxidized products, possibly using the catalyst itself as an adsorbent, or some other solid-phase adsorbent. In a recent study using both a solid catalyst and oxidant,⁴⁴ the ODS of organosulfur compounds of peroxycarboxylic-acid-functionalized hexagonal mesoporous silica (HMS) has been investigated. The organosulfur compounds (representatives of those contained in the light and medium distillates), were dissolved in an aromatic solvent (toulune). After 2 h reaction, 97% of DBT and 47 % of BT was removed at 343 K and atmospheric pressure for a peroxycarboxylic acid groups on catalyst to sulfur ratio of 3.

1.9 The Goal of this Research Work

In the present work, we have studied oxidation of the model compounds thiophene , dibenzothiophene, acridine and carbazole in a model diesel using oxygen . In particular, Pd/carbon and MoC/ Al_2O_3 catalysts were synthesized and proven to demonstrate a superior activity and (sometimes) selectivity toward oxidation of organosulfur and organonitrogen compounds, when compared to Co-, Pt-, Cu- and heteropolyacid-supported catalysts. The

study was conducted on a synthetic mixture of heterocyclic sulfur, heterocyclic nitrogen, alkylaromatic and aliphatic compounds representative of those contained in number 2 diesel. The catalysts were characterized by measuring dispersion and surface area, and the major oxidation products were identified. Potential mass transfer limitations on the reactions were analyzed.

CHAPTER 2 EXPERIMENTAL METHODS

2.1 Catalyst Preparation

Eight supported Pd, Mo₂C and WC catalysts were synthesized. These were (nominal compositions, wt%) CDX1 (11.1% Mo₂C/Al₂O₃), CDX2 (10.5% Mo₂C/AC), CDX3 (10.5% Mo₂C/AC), CDX4 (11.3% WC/Al₂O₃), CDX5 (4% Pd/Al₂O₃), CDX6 (4% Pd/Al₂O₃), CDX7 (5% Pd/OMC) and CDX8 (5% Pd/OMC), where AC is activated carbon and OMC is an ordered mesoporous carbon.

CDX1 were prepared according to Mariadassou et. al.⁴⁵ Catalox HTA-101 alumina (Sasol, 0.002% Na₂O, 75-115 m²/g, 0.70 mL/g pore volume, 24-34 nm pore diameters) was calcined at 573 K for 3 h in 200 mL/min air (Capitol Welders, Industrial grade). The temperature was ramped from room temperature (RT) to 573 K at 5 K/min. Ammonium molybdate hydrate (AMH, 81.5% MoO₃, Baker, ACS Reagent) was dissolved in DI water (0.253 g/mL). The calcined alumina was impregnated with aqueous AMH solution dropwise (0.357 mL/g support), then dried at 373 K overnight in air and calcined at from 423-773 K in 210 mL/min air; the entire impregnation/drying process was then repeated. Finally, the material was carbonized by treatment with flowing N₂ (Capitol Welders, UHP grade, 200 mL/min) at 393-673 K at 2 K/min with a 1 h hold, then in a flowing CH₄/H₂ mixture (170 mL/min, AirGas, 19.9 vol% ± 1% CH₄) at from 673-1123 K at 0.5 K/min and held for 3 h. After cooling down to room temperature in 200 mL/min of H₂, the sample was passivated in 200 mL/min of O₂/N₂ (1 vol%/99 vol%) for 1 h.

CDX2 was prepared according to Mariadassou et. al.,⁴⁶ and Hercules et. al.⁴⁷ The carbon pretreatments for CDX2 and CDX3 were adapted from Rao et al.,⁴⁸ Furmanek et al.⁴⁹, Rao and Weigert⁵⁰. Calgon PCB 6X16 (manufacturer specifications: coconut shell-based, $\rho_b = 0.41$ g/mL, 1100 m²/g, 1% ash, 3% moisture maximum) activated carbon was washed with 1 M HNO₃ overnight with gentle stirring, then with DI water until the pH of the washings was

> 4; then the previous two steps were repeated until the pH of the washings was > 5. The carbon was dried at 393 K, then calcined at 300°C for 3 h in static air, then impregnated with aqueous AMH solution (0.204 g/mL) dropwise at RT, while stirring with a Teflon rod. The sample was then dried in static air at 393 K overnight, then calcined at 773 K for 2 h in flowing N₂ (300 mL/min), then switched to flowing H₂ (300 mL/min), and ramped from 773-973 K at 1 K/min, with a 1.5 h final hold. Then the flow was switched to N₂ while cooling to RT, and finally the sample was passivated for 1 h with 1 vol% O₂/N₂.

CDX3 was prepared according to literature.⁴⁶ The Calgon carbon was treated as with CDX2, but 1 M HF was substituted for HNO₃ in the second acid treatment, which lasted for 48 h at RT, followed by washing with DI water until the pH of the washings was > 5. The carbon was then dried at 393 K and calcined at 573 K for 3 h in static air. It was then impregnated with AMH solution (0.204 g/mL) dropwise at RT while stirring with a Teflon rod. The sample was then dried, calcined and carbonized in the same manner as CDX2.

CDX4 was synthesized according to the literature.⁵¹ Catalox HTA-101 alumina was calcined at 573 K for 3 h in 200 mL/min flowing air. It was then impregnated (0.454 g solution/g support) dropwise with ammonium metatungstate (AMT, AlfarAesar, 99.99% on a metals basis) aqueous solution (0.366 g/mL) while stirring. The material was then dried at 373 K overnight in static air, calcined in 200 mL/min flowing N₂ at from 373-773 K, 2 K/min with a 6 h final hold. The remainder of the synthesis is the same as for CDX2 except the final carbonization was at 1123 K for 3 h.

CDX5 was made according to literature.⁵² To calcined Catalox HTA-101 alumina was added aqueous Pd(NO₃)₂ (Fluka, ≥95%) solution (9.1% salt, 1 mL/g support) dropwise, with stirring by a Teflon rod. A separate aqueous hydrazine solution of 0.13 g/mL of 81% hydrazine hydrate (Acros, 99.5%) was then added to the impregnated material to reduce and deposit the Pd on the support, while evaporating excess water. The sample was then dried at

393 K overnight and calcined at 773 K in 40 mL/min of air for 3 h, then cooled to 448 K in 40 mL/min of N₂, and finally reduced at 448 K in 50 mL/min of 20 vol% H₂/N₂ for 2 h.

CDX6 was prepared according to Rahaman and Vannice.⁵³ The PdCl₂ (Acros, 59% Pd) was dissolved in HCl and evaporated to near dryness twice, adding distilled deionized water to obtain the required volume of solution (6.5% salt). To calcined Sasol HTA-101 alumina was added aqueous PdCl₂ solution (1 mL/g support) dropwise, with stirring by a Teflon rod. The sample was then dried at 393 K overnight and calcined at 393 K in 300 mL/min of N₂ for 1 h. After that it was reduced at 393 K for 1 h and then at 448 K for 1 h in 345 mL/min of 15 vol% H₂/N₂. Under the same atmosphere, the sample was cool down to RT.

Synthesis of the organic mesoporous carbon (OMC-3) was adapted from Dai and co-workers.⁵⁴ To equal weights of resorcinol (Acros, 98%) and BASF F-127 copolymer (ethylene oxide-propylene oxide) was added 4.09 mL/g ethanol and 4.09 mL/g 3.0 M HCl. Then 37% aqueous formaldehyde was added in a 1.18 wt ratio with stirring at RT until phase separation (<40 min). After phase separation, the gel was centrifuged, stirred for another 40 min, then dried at 353 K for 24 h and 393 K for 24 h. Carbonization was with flowing N₂ (300 mL/min), 1 K/min from 393 K to 673 K, 2 h hold, , then 5 K/min from 400 K to 850 K, 3 h final hold.

To prepare CDX7,^{55,56} PdCl₂ (Acros, 59% Pd) was dissolved in about 200 mL of 0.1 M HCl per g PdCl₂, with gentle heating. After cooling to RT, the appropriate amount of this solution was added to dry OMC-3 carbon to get 5% nominal loading of Pd, with stirring. Then 0.1 M NaOH was added to bring the pH to 12, stirring for 3 h. The material was filtered, washed with water several times until the pH of the washings was < 9, dried at ~373 K overnight, then finally reduced at 523 K for 3 h, with a 5 K/min ramp from 373 K, in 10 vol% H₂/N₂. To prepare CDX 8,⁵⁶ to an aqueous K₂PdCl₄ (Sigma Aldrich, 98%) solution (0.3265 g/mL), 5 mL/mL of aqueous 2% PVA (Kodak, 99-100% hydrolyzed, Reagent Grade)

solution, 200 mL/mL of DI water and 20 mL/mL of aqueous NaBH₄ (Acros, 98%) solution (3.78 g/L) were added, respectively. Then 0.1M H₂SO₄ was added to bring the pH to 3. A proper amount of OMC-3 carbon was added to the solution in order to get 5% nominal loading of Pd. The carbon contacted the solution overnight, with stirring, after which the material was filtered, washed with water several times until the pH of the washings was < 9, dried at ~373 K overnight, then finally reduced at 523 K for 3 h, with a 5 K/min ramp from 373 K, in 10 vol% H₂/N₂.

2.2 Semibatch Reactor Experiments

The reactions were carried out in 20 mL (total heated volume) 316 stainless steel semibatch reactors with a ¼" ball valve to connect them to an O₂ (Capitol Welders, Industrial grade) cylinder (see Figure 2.1). Four of these reactors were loaded into a heating block with insulation around their tops. A K-type thermocouple was mounted into the center slot of the heating block; temperature was controlled by a PID controller, and was usually within ± 1 K of the set point. A typical catalyst load was 0.1g. Some catalysts were pretreated in situ under a reducing atmosphere before the reaction, and then purged with N₂. After that, 10 mL of a model number 2 diesel (75 wt% hexadecane (Aldrich, 99%), 12 wt% ethylbenzene (Fisher,98%), 12 wt% 1-methylnaphthalene (Aldrich, 98%), 0.03 wt% carbazole (Aldrich, 99%), 0.02 wt% acridine (Kodak, 99%), 0.4 wt% thiophene (MCB,99%), and 0.55 wt% DBT (Aldrich, 98%)) was loaded into the reactors. Then the system was flushed with O₂ at the desired pressure three times and the rocking mechanism for the reactor block started at ~60 rpm. Once the reactors rose to the desired reaction temperature, the valves were left open to the O₂ cylinder. When the final time was reached, all valves were shut off, the rocker was stopped, and the reactors were removed and cooled.

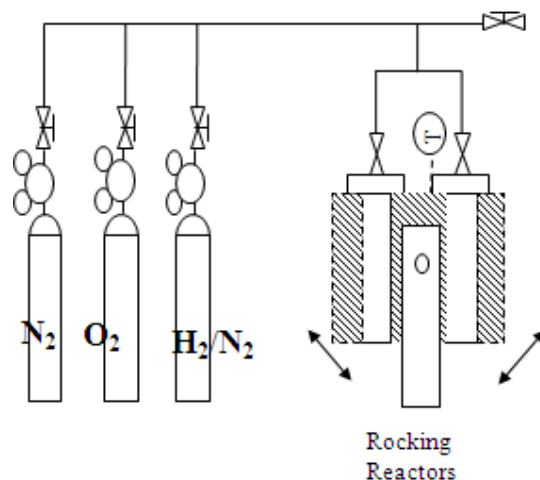


Figure 2.1 Schematic of semibatch reactor system

2.3 Analysis of Product Samples

Two samples were removed from each reactor, each 4 mL. One sample was used for quantitative GC analysis of how much of the initial compounds had reacted; the other sample was saved for qualitative GC-MS analysis to identify products. For quantitative GC, the 4 mL sample was mixed with 40 μ l mesitylene (used as internal standard), and then stored in a refrigerator until use.

These samples were injected into an HP-5890 II GC fitted with a flame ionization detector (FID), using an HP-7673 autosampler. An Alltech EC1 column (30 m length, 0.32 mm ID) was used to separate the compounds. Further details on the analysis and the calibration can be found in Appendix A.

A few samples were analyzed using a 5890 II GC with an H-P 5972 electron impact mass spectrometric detector. These samples were separated using an SP-2380 (Supelco) column, 30 m long, 0.25 mm id, 0.20 micron film thickness, at 373-403 K, 10 K/min, with at least 15 min final hold time. Compound identifications were made using either the NBS or Wiley compound libraries.

2.4 Catalyst Characterization

Dispersions of Pd-containing catalysts were estimated based on H₂ pulse chemisorptions using a Micromeritics 2700 unit. All catalysts were pretreated in situ before being exposed to fixed-volume pulses of H₂ at RT. The pretreatment methods can be found in Table D 4-8 of Appendix D. The assumed adsorption stoichiometry for hydrogen chemisorptions was 0.5 mol H₂/mol active metal.

BET surface areas and pore size distributions (PSD) were obtained from N₂ adsorption-desorption isotherms using a Quantachrome AS-1, after at least 30 min of drying under vacuum at 300 K. Elemental analyses for Pd were by inductively coupled plasma - atomic emission spectroscopy (ICP-AES), after dissolving the Pd catalysts in boiling concentrated HNO₃ three times. The contact pHs of carbons and catalysts were measured by mixing the solid with DI water (1 g/10 mL). Prior to the measuring the pH of the suspension, the pH meter (pH8500, Sargent-Welch) was calibrated with two buffer solutions (pH=4 and pH=8).

2.5 Coating of Monoliths for Future Work.

The carbon support (Calgon PCB 6X16) was treated by washing with 1 M HNO₃ overnight with gentle stirring. The acid-treated carbon was then washed with DI water until the pH of the washings was > 4. The previous two steps were repeated until the pH was > 5. Then the carbon was ground in a porcelain mortar and pestle to >200 mesh.

Three methods were tested to coat carbon onto the monoliths. Before coating, the monoliths (200 cpsi, 5 × 5 × 1.2 cm, 1.3 mm hole diameter) were boiled in DI water for 3 h to clean impurities from the surfaces. All three methods used freshly polymerized resin to bind particulate carbon to the monoliths. The desired total carbon loading was 5%. Method 1 used polymerized sucrose (sample CMN-1), method 2 used furfuryl alcohol-furan copolymer (CMN-2), and method 3 formaldehyde-resorcinol copolymer with F-127 (PO-EO copolymer, 106/70 PO/EO, BASF) template (CMN-3). Some of the final carbon coating was scratched

from the monoliths and analyzed by N₂ adsorption in a Quantachrome AS-1 physisorption instrument by the 3-point BET method.

Method 1 was adapted from Ryoo and coworkers,⁵⁷ Jaroniec et. al.,⁵⁸ and Sakintuna and Yurum.⁵⁹ A 0.03 H₂SO₄/0.24 sucrose (Fisher, 99.8%)/H₂O (wt ratio) solution was stirred for 1 h at RT to polymerize the sucrose, then 0.75 wt ratio to H₂O of the carbon with stirring for 30 min. The monolith was coated by pipetting slurry into the holes, and drying it at 373 K for 2 h, in a vertical position. Any holes totally blocked by carbon were freed by a syringe needle, and the carbon on the top and sides was scraped off. The coated monolith was then weighed, and if the loading was insufficient coated again. These last two steps were also followed in methods 2 and 3. It was then calcined in N₂ (300 mL/min) at from RT to 1123 K at 5 K /min with a 3 h final hold.

Method 2 was adapted from Garcia-Bordeje et. al.⁶⁰ For every 1 g carbon, 2 g acetone (reagent, Fisher), 3.2 g furfuryl alcohol (99%, Aldrich) and 4.8 g partly polymerized furan resin. were homogenized, then the carbon and 0.1 g HNO₃ (polymerization catalyst) added. After stirring for 30 min, the monolith was dipcoated in the mixture, dried at RT overnight, then at 373 K for 2 h. It was then calcined in N₂ (300 mL/min) at from RT to 1123 K at 5 K /min with a 3 h final hold.

Method 3 was adapted from Dai and coworkers.⁵⁴ Equal weights of resorcinol (Acros , 98%) and F-127 copolymer were dissolved in 4/1 (wt) ethanol (absolute, reagent, Sigma-Aldrich) and 4/1 3 M HCl. Then, while stirring, formaldehyde solution (37% in water, MCB) was added drop by drop at a vol/vol ethanol ratio of 0.27. The solution was stirred at RT for 40 min, becoming turbid. The gel phase was centrifuged, and then mixed with 1 wt carbon/4 wt gel, stirring with a teflon rod. The slurry was then manually pushed into the holes of the monolith, using compressed air and/or a needle to remove excess gel. The monolith was dried at 353 K for 24 h and 393 K for 24 h, then calcined in flowing N₂ at 393-673 K, 1 K/min with

a 3 h hold, then ramped from 673 to 1123 K at 5 K/min with a 3 h final hold. The above steps were repeated until the desired loading of carbon was reached.

CHAPTER 3 RESULTS AND DISCUSSION

3.1 Catalyst Characterization Results

For the synthesized mesoporous carbon OMC-3, the BET surface area was 680 m²/g. The BJH pore size distribution of the OMC was also measured based on the adsorption isotherm. The average pore diameter was 4.90 nm by assuming cylindrical geometry. The average pore radius r can be obtained as:

$$r = \frac{2V_q}{S}. \quad [\text{Eq. 3.1}]$$

$$\text{With } V_q = \frac{P_a \times V_{\text{ads}} \times V_m}{RT} \quad [\text{Eq. 3.2}]$$

where V_m is the molar volume of the liquid adsorbate (34.7 cm³/mol for N₂), P_a and T are ambient pressure and boiling point of liquid N₂; V_{ads} is the volume of N₂ adsorbed, and S is the BET surface area. The pore size distribution (PSD) plot for the OMC-3 is in Figure 3.1. From the pore size distribution, a better estimate of the average pore diameter (6.5 nm) can be obtained from the equation $D_a = \frac{\int D \times S(D) dD}{\int S(D) dD}$, where D_a is the average pore diameter, D is the pore diameter and $S(D)$ is the surface area of a pore with a diameter $D + dD$. The surface area, average pore diameter and PSD for OMC-3 are very close to the values (specific surface area ~ 600 m²/g, pore size ~ 6.3 nm) reported in the literature for this same synthesis.⁵⁴

Pd weight loadings on the Pd/OMC catalysts CDX7 and CDX8 were determined by ICP-AES; these results are summarized in Table 3.1. Metal dispersion was measured on a Micromeritics 2700 by pulse chemisorption of H₂. From the chemisorption and Pd loading results, we can conclude that the deposition and precipitation method used in the preparation of CDX7 has a higher dispersion and Pd utilization efficiency. To ensure the validity of these measurements, the dispersion tests were repeated twice. Also the BET surface areas and dispersions determined by chemisorptions of H₂ on a Micromeritics 2700 for some of the catalysts used here, and are summarized in Table 3.2.

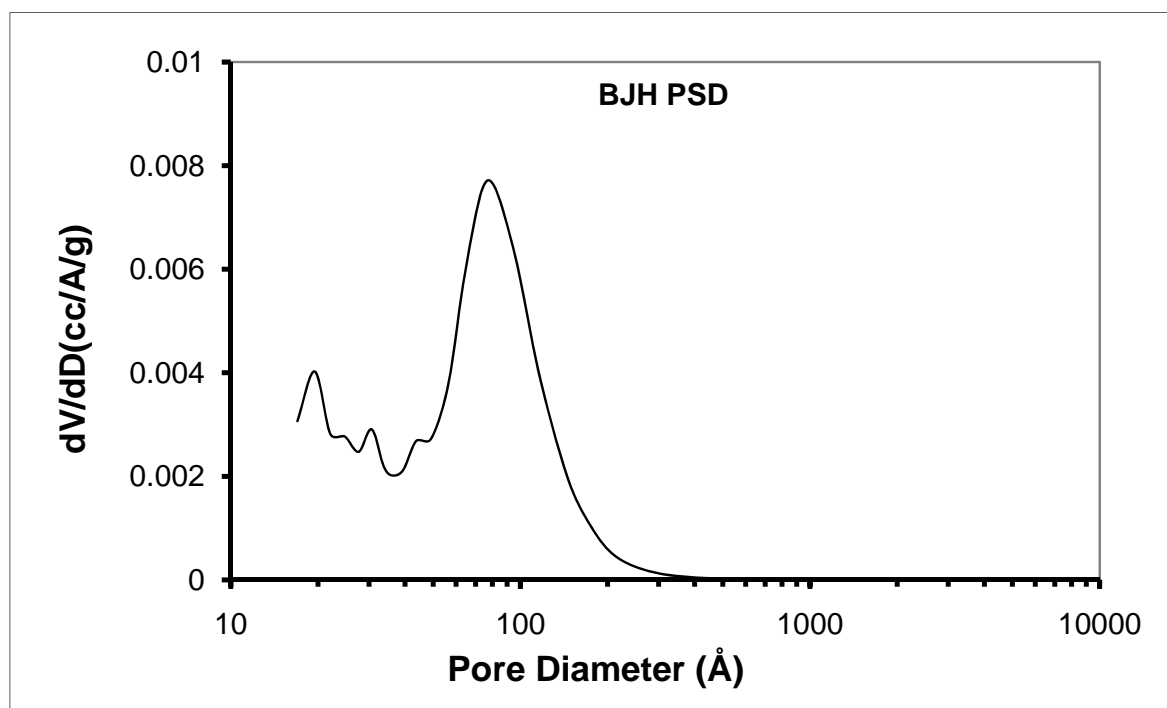


Figure 3.1 The Pore Size Distribution for OMC-3

Table 3.1 Characterization of CDX7 and CDX8 catalysts

Catalyst	Pd loading (%)		Standard Deviation	Dispersion (%)		Standard Deviation
CDX7	3.8%	3.9%	0.05%	78%	77%	1.06%
CDX8	3.0%			30%	28%	1.13%

The specific surface areas, average pore sizes and pore volumes of the carbon washcoats on the coated monoliths are shown in Table 3.3. The average pore diameters were obtained through the simpler average formula [3.1]. From just a surface area perspective, CMN-1 is superior to CMN-3. However, the carbon washcoat of CMN-1 is less strongly bound to the monolith and easier to remove. So we can conclude that the resorcinol-formaldehyde-copolymer gel method used to prepare CMN-3 is probably the best method we found to coat carbon to a monolith, although the sucrose polymerization gives a much larger average pore size.

Table 3.2 BET surface areas and dispersions of catalysts

Catalyst	BET Surface Area (m ² /g)	Dispersion (%)
5% Pd/Eng	1100	35
5% Pd/MPT-5	800	29
5% Pd/Deg	715 ⁶¹	29
CDX1	70	
CDX2	790	
CDX3	840	
CDX4	90	
CDX5		56
CDX6		9.3
CDX7		79
CDX8		31
CsHPW/SiO ₂	130	
Pt-S2		50

Table 3.3 Physical characterization of carbons removed from monoliths

Carbon	Specific Surface Area (m ² /g)	Average Pore Size (nm)	Pore Volume (cc/g)
CMN-1	750	29	0.45
CMN-2	180	3.0	0.014
CMN-3	630	3.9	0.62

The contact pH values for the commercial 5% Pd/carbon catalysts, OMC-3 and the Calgon PCB carbon used to make the CMN series of catalysts are given in Table 3.4. Clearly the 5% Pd/MPT-5 catalyst is relatively neutral while the other two commercial catalysts are weakly basic. Weakly basic sites on activated carbons typically result from high temperature carbonizations in inert gas or under vacuum, which strip oxygen-containing groups from the surface.⁶² The interaction of water with the graphitic carbon basal planes is presumed to generate surface OH⁻ groups.

Table 3.4 Contact pH for Pd/carbon catalysts.

	5%Pd/MPT-5	5%Pd/Deg	5%Pd/Eng	OMC-3	Calgon PCB
pH	7.0	8.2	9.3	8.5	10.4

3.2 Analysis of Oxidation Products

To determine the reaction products, only the samples with maximum conversion of S-heterocycles and N-heterocycles were analyzed by GC-MS. Based on the molecular fragmentation patterns, we identified principal oxidation products from certain feed compounds. These products are summarized in Table 3.5. The exact identity of the nitroso compounds could not be determined.

Table 3.5 Oxidation products identified by GC-MS

Substrate	Oxidation Product
ethylbenzene	acetophenone, 1-phenylethanol
1-methylnaphthalene	naphthalenecarboxaldehyde
DBT	DBT sulfoxide,
acridine, carbazole	nitroso compounds
acridine	methylquinoline

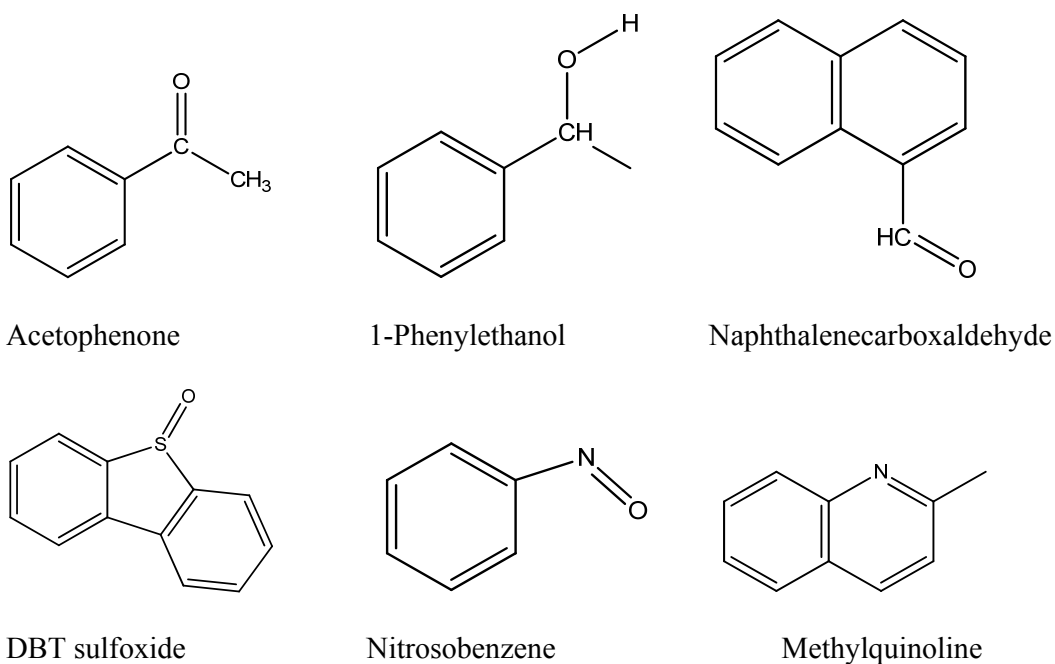


Figure 3.2 The Chemical Structures of Oxidation Products

From the analysis of the products, we can conclude that both oxidation and cracking reactions take place in these experiments. There were traces of DBT sulfoxide and of a nitroso compound, which was formed from either acridine and carbazole. There was also evidence of a methylquinoline, which can be formed by the cracking of acridine. However, the concentration of products from oxidation of the N-heterocycles is very low, because the feed concentrations are themselves low. Therefore, product samples from larger batches are needed to pin down the exact structures. These experiments will be done in the future using a reactor of 1 L capacity.

According to the literature, the main products from oxidation of DBT and thiophene should be the corresponding sulfones.⁷ DBT and thiophene are oxidized first to the sulfoxides, then further oxidized to the sulfones. The rates of oxidation are first order in concentration.⁶³ The rate to sulfone from sulfoxide is typically higher than the rate at which the sulfoxide is formed.³⁰

The absence of sulfones and the almost complete absence of sulfoxides (only one small peak in one sample) suggests that almost all sulfones were formed, which were then adsorbed by the catalysts themselves. The catalyst supports have polar or moderately polar surface groups which are present in quantities sufficient to adsorb the sulfones produced. Typical sulfur and nitrogen concentrations (S: 6.23×10^{-3} mol/L; N: 4.65×10^{-4} mol/L) compare to total catalyst adsorption site concentrations (based on $N_2 = 0.162 \text{ nm}^2$) of 8.2×10^{-3} mol/g (800 m^2/g) and 1.0×10^{-3} mol/g (100 m^2/g). It is reported that the concentration of acidic adsorption sites on the surface of Calgon BPL activated carbon is 0.847 meq/g.⁶⁴ For a typical 0.1 g load of catalyst in each experiment, the amount of acidic adsorption sites on the carbon is 8.47×10^{-5} mol. Even if all the S-heterocycles in the feed stream had been converted into sulfones, the amount of acidic sites (8.47×10^{-5} mol) is still larger than the amount of sulfones (6.23×10^{-5} mol), and if other sites participated in the adsorption the S/site ratio is smaller for carbons, and still < 1 for the other supports (e.g., 0.62 for a 100 m^2/g support based on N_2 adsorption). The sulfoxides and sulfones are weakly basic.⁶⁵ If the surface of the support is either mildly acid (e.g., SiO_2) or neutral (the commercial carbons and most commercial aluminas), then most of the sulfones and sulfoxides could be adsorbed on the surface of the catalyst and its support. It is also reported that product sulfones and sulfoxide are adsorbed on the surfaces of catalysts, e.g., with amorphous $\text{TiO}_2\text{-SiO}_2$.⁶⁶

Of course, more than just sulfones and sulfoxides can be adsorbed on catalyst surfaces. It was reported that the selectivity of adsorption on the activated carbon Nuchar SA 20 (surface area= 1843 m^2/g and average pore diameter = 2.86 nm) for various organics increased in the order: naphthalene ($\alpha_{j,n} = 1.0$, selectivity relative to naphthalene) $<$ 1-methylnaphthalene ($\alpha_{j,n} = 1.3$) $<$ DBT ($\alpha_{j,n} = 3.0$) $<$ 4,6-DMDBT ($\alpha_{j,n} = 4.5$) $<$ quinoline ($\alpha_{j,n} = 8.1$) $<$ indole ($\alpha_{j,n} = 10.6$).⁶⁷ The authors suggested that the methyl group on the aromatic ring enhances its adsorption affinity due to an increase in π -electron density on the aromatic rings,

through electron donation. As for quinoline and indole, indole can interact with both acidic (such as carboxyl and phenol groups) and basic (such as ketone and chromene groups) oxygen functional groups on the carbon surface, while quinioline can interact only with the acidic groups, leading to higher adsorption selectivity for indole.

The oxidation of ethylbenzene with O₂ is likely to produce ethylbenzene hydroperoxide (EBHP) in situ, along with the stable products acetophenone and 1-phenylethanol.⁶⁸ After 4 h oxidation using 70% O₂ at 403K, the conversion of ethylbenzene was ~12%.⁶⁸ In one of our experiments with 5%Pd/MPT-5, the conversion of ethylbenzene was 9.5% under pure oxygen at 343 K for 4 h. Although EBHP was not identified by GC-MS in the product sample, it is known to be unstable and typically decomposes to 1-phenylethanol in a heated injection port of a GC. Also, it is well known that organic peroxides can oxidize DBT and thiophene to sulfoxides and sulfones even at room temperature with various catalysts.⁶⁹ The 1-methylnaphthalene can be converted to endoperoxides using O₂ in a photocatalytic reaction.⁷⁰ This peroxide could decompose to an aldehyde or an alcohol; naphthalenecarboxaldehyde was observed here.

The literature on the oxidation of acridine is sparse. One study dealt with its electrochemical oxidation, and here acridine polymers were obtained.⁷¹ It is reported that carbazole-1,4-dione can be obtained by the oxidation of carbazole with H₂O₂, catalyzed by a titanosilicate.⁷² Carbazole can also be converted into 3-hydroxycarbazole or 2'-aminobiphenyl-2,3-diol under the action of some specific enzymes,^{73,74} or can form polymers by electrochemical oxidation, similar to acridine.⁷⁵ It was found recently that carbazole can be converted into a polymer containing C=O and -OH groups when oxidized with H₂O₂ over a vanadosilicate.⁷⁶ The lack of identifiable products from the oxidations in this work suggests that polymerization may have taken place. If so, NMR studies of larger samples may be necessary to determine the product distribution.

3.3 Activity and Selectivity of the Catalysts

Through the integration of the chromatograms, the ratio of areas between peak *i* and peak *s* (mesitylene standard) can be obtained. Then the conversion of each compound in the sample can be calculated.

$$X_i = \frac{\frac{C_i^0}{C_s^0} - f_i \times \frac{A_i}{A_s}}{\frac{C_i^0}{C_s^0}} \quad \text{Equation 3.3}$$

In Equation 3.1, A_i is the peak area of compound *i*, while A_s is the peak area of internal standard *s*. C_i^0 is the molar concentration of compound *i* and C_s^0 is the molar concentration of internal standard *s*. The f_i is the calibration factor of compound *i*.

The key selectivities (S oxidation relative to alkylaromatic oxidation, and N oxidation relative to alkylaromatic oxidation) were quantified as scatter plots for the various series of catalysts to determine if there were common trends; the series are the base metals, heteropolyacids, Pt group, metal carbides, and the Pd group.

The molar amount of reacted S-heterocycles (N_S) was calculated as:

$$N_S = N_{\text{thiophene}}^0 \times X_{\text{thiophene}} + N_{\text{DBT}}^0 \times X_{\text{DBT}}$$

where N^0 is a molar amount of feed, and X is a fractional conversion.

The molar amount of reacted N-heterocycles (N_N) was calculated as:

$$N_N = N_{\text{acridine}}^0 \times X_{\text{acridine}} + N_{\text{carbazole}}^0 \times X_{\text{carbazole}}$$

The molar amount of reacted alkylaromatics (N_A) was calculated as:

$$N_A = N_{\text{ethylbenzene}}^0 \times X_{\text{ethylbenzene}} + N_{\text{1-methylnaphthalene}}^0 \times X_{\text{1-methylnaphthalene}}$$

3.3.1 Base Metal Catalysts

The base metal catalysts used in these experiments were CoSi1 (8% Co/aminated SiO₂), ReSi1 (~10% Re/SiO₂), 7.9% CuO/TiO₂ and ZC-1(60% acid site exchanged Linde Y zeolite, exchanged with Co²⁺). These are all catalysts for hydrocarbon oxidation. From Figs. 3.3 and 3.4 we can conclude that the 7.9% CuO/TiO₂ and ZC-1 are almost inactive for the oxidation

of S-heterocycles, N-heterocycles and alkylaromatics. From Fig 3.3, it is concluded that CoSi1 and ReSi1 behaved similarly in the oxidation of S-heterocycles. The point at the far right was taken at a much higher pressure than normal for these runs, 1.83 MPa. But the same trend is followed. The curve for ReSi1 is slightly above the curve for CoSi1 in Fig 3.3, and below that of ReSi1 in Fig 3.4. Therefore ReSi1 is slightly more selective for the oxidation of S-heterocycles, while for both catalysts the oxidation of the alkylaromatics inhibits the oxidation of the N-heterocycles. The obvious explanation for the inhibition is that the sites for conversion of the N-heterocycles are poisoned by the products of alkylaromatics oxidation. As the reaction temperature and pressure of O₂ increased, the amount of alkylaromatics and S-heterocycles reacted increased for ReSi1. But for CoSi1, the narrow temperature range used here (343-363 K) did not have an obvious effect on the oxidation of the S-heterocycles.

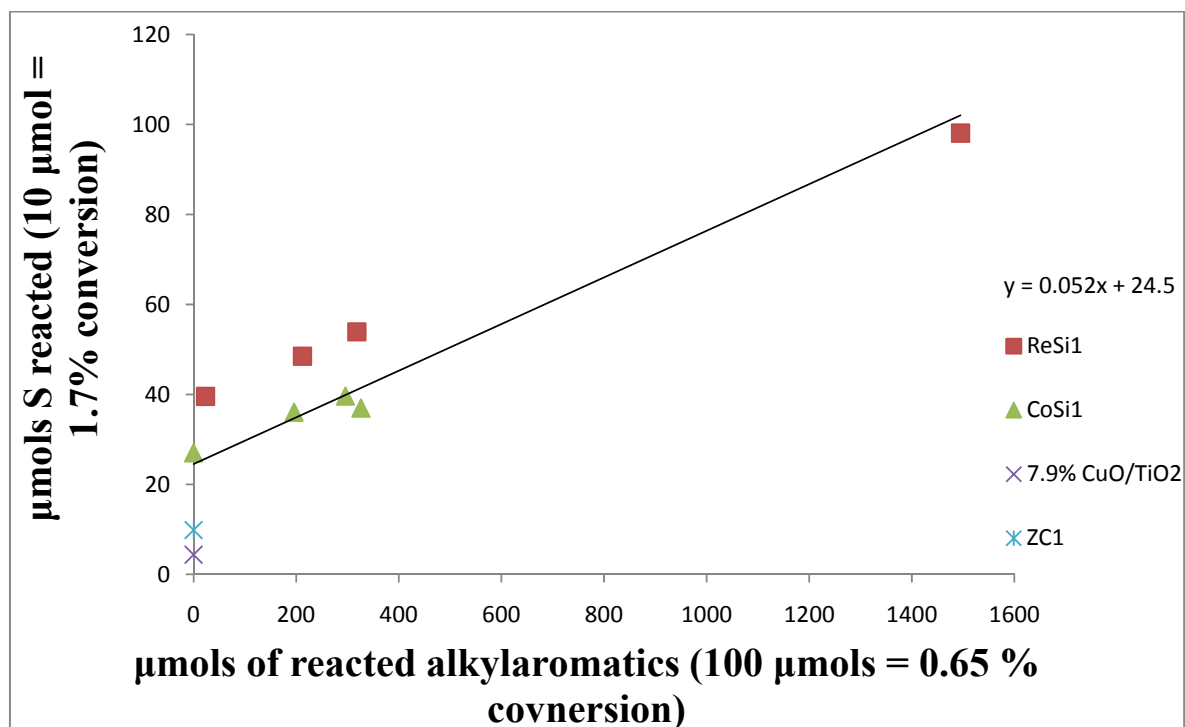


Figure 3.3 Selectivity of base metal catalysts for S-heterocycles

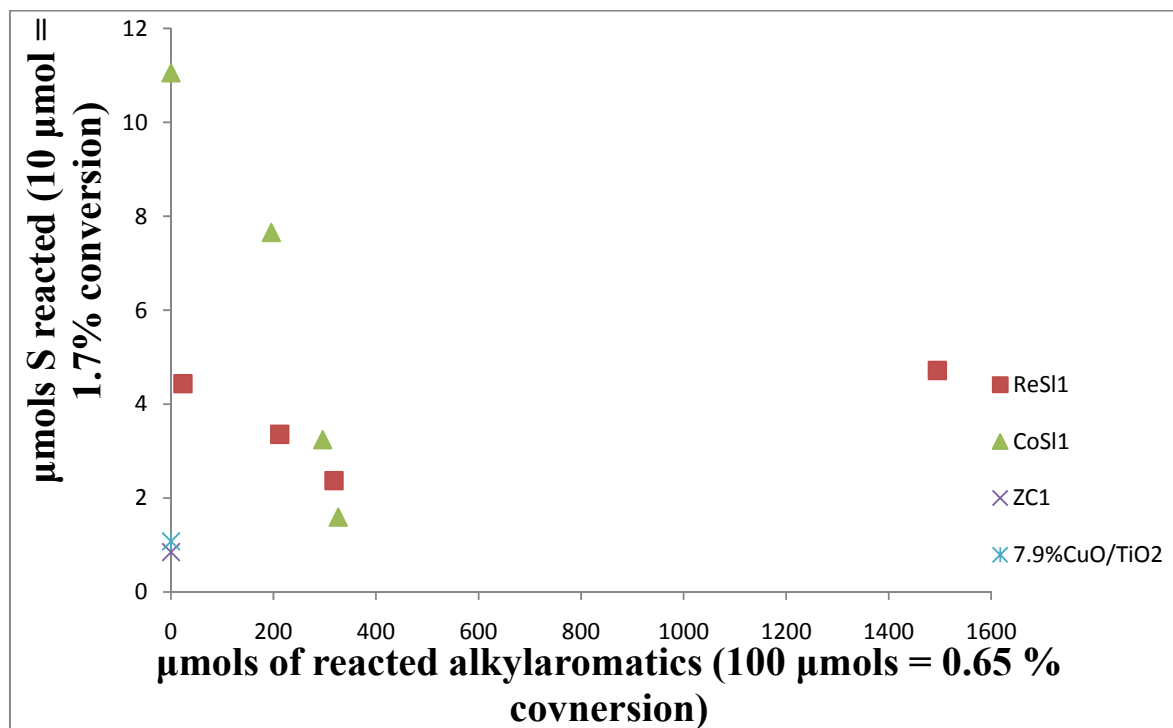


Figure 3.4 Selectivity of base metal catalysts for N-heterocycles

3.3.2 Heteropolyacid Catalysts

The heteropolyacid catalysts tested included 0.01 g per mL feed of CsHPW-SiO₂ (Cs_{2.5}H_{0.5}PW₁₂O₄₀·6H₂O(40 wt%)/SiO₂), 0.03 g per mL feed of Cs_{2.5}H_{0.5}PW₁₂O₄₀, 0.03 g per mL feed of (NH₄)₃H₂PMo₁₂O₄₀, 0.03 g per mL feed of (NH₄)₅H₄PV₆W₆O₄₀ and 0.03 g per mL feed of Cs_{2.5}Ni_{0.08}H_{0.34}PMo₁₂O₄₀. The different weights were used to adjust the catalyst surface areas to more similar amounts. Almost all these experiments were at the same reaction conditions, 363 K and 0.79 MPa of O₂ for 2 h. Two experiments using CsHPW-SiO₂ were at 343 K and 0.58 MPa of O₂ for 2 h. As we can see from the Fig 3.5, the amount of reacted S-heterocycles again increased with the amount of reacted alkylaromatics for the heteropolyacid catalysts, same as for the base metal catalysts. Again, the amount of reacted N-heterocycles decreased as the amount of reacted alkylaromatics increased, so the active sites for reaction of N-heterocycles were poisoned by the products of oxidation of the alkylaromatics. It can be concluded that there are two different types of active sites for the

heteropolyacid and supported base metal catalysts CoSi1 and ReSi1. While in general the heteropolyacids are less selective for S-heterocycle oxidation than CoSi1 or ReSi1 (compare Figs. 3.3 and 3.5), the supported CsHPW-SiO₂ may be more active for oxidation of S-heterocycles than either the unsupported heteropolyacids or the base metal catalysts, although the evidence is limited. A similar phenomenon was reported by Ishii et al.⁷⁷ in the oxidation of benzylic alcohols by O₂ catalyzed by activated carbon-supported (10%) (NH₄)₅H₆PMo₄V₈O₄₀. They found that the catalyst showed high activity to the aldehydes in toluene solvent, while the unsupported catalyst was inactive at the same conditions. The enhancement of catalytic activity by the support was believed to be due to the higher concentration of substrates and oxygen by adsorption in the vicinity of the active site.

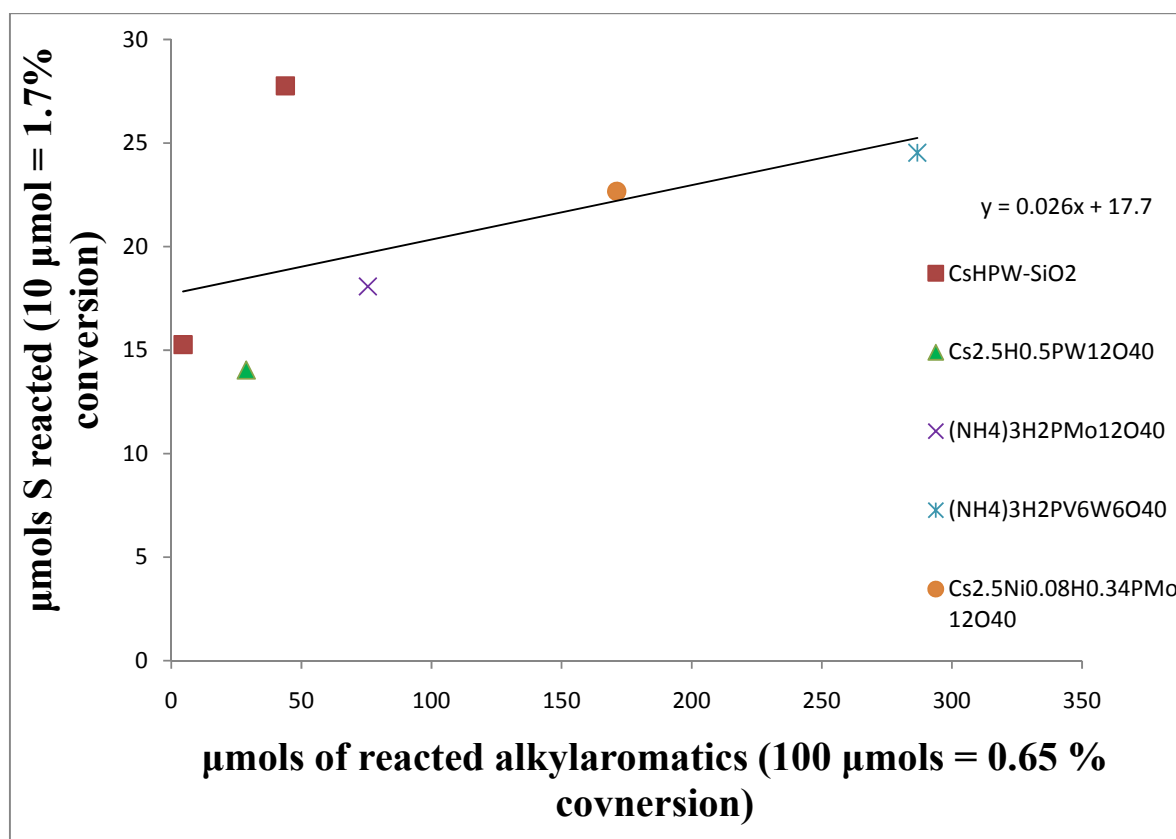


Figure 3.5 Selectivity of heteropolyacid group catalysts for S-heterocycles

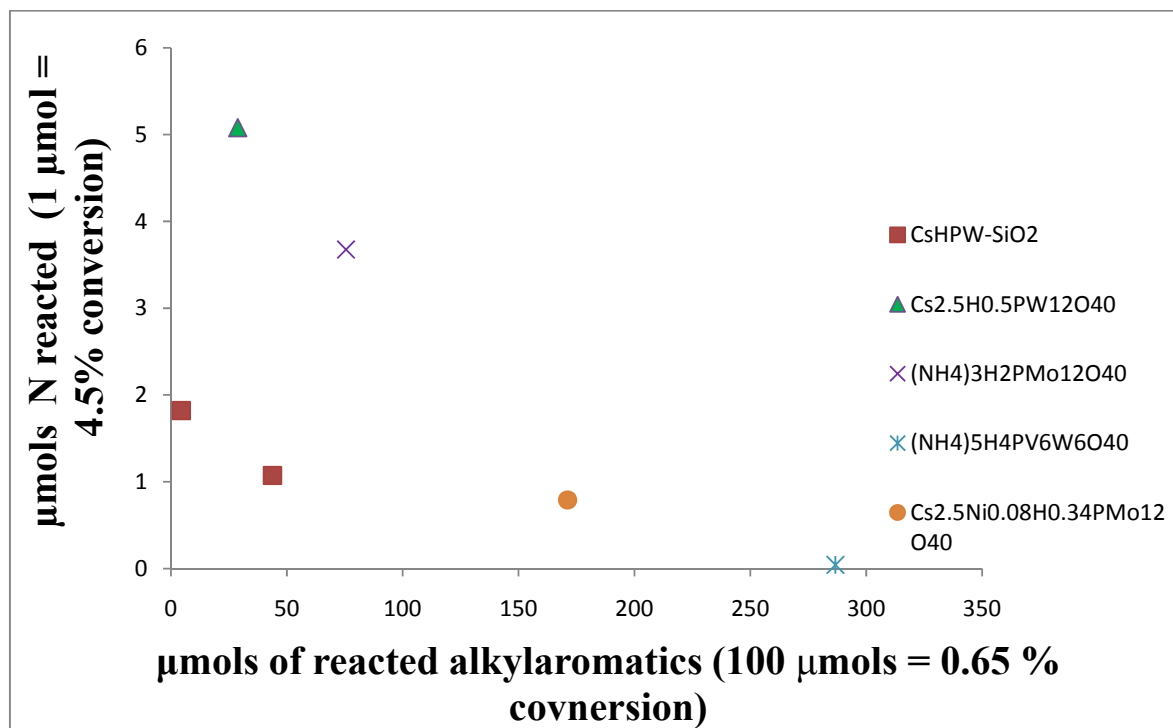


Figure 3.6 Selectivity of heteropolyacid group catalysts for N-heterocycles

3.3.3 Pt-based Catalysts

For the Pt-based catalysts, one experiment each with Pt-S2 and 1% Pt/Zn/K/Al₂O₃ were carried at 343K, 0.79 MPa for 4 h and one experiment with 0.5% Pt/Al₂O₃(Aldrich) was carried out at 343K, 0.79 MPa for 2 h. The Pt group behaves similar to the base metals in the oxidation of S-heterocycles (compare Figs. 3.7 and 3.3). However, the N-heterocycle vs. alkylaromatic relationship is dissimilar. In particular there is no apparent inhibition by the alkylaromatic oxidation products. Pt-S2 performed slightly better than other two Pt catalysts, probably due to its higher Pt loading (3%).

3.3.4 Carbide Catalysts

The carbide catalysts tested included Mo₂C supported on activated carbon (CDX2 and CDX3) and WC on alumina (CDX4). The experiments for the carbide catalysts were at 343K and either 0.79, 1.14, or 1.83 MPa for 4 h. From Figs. 3.8 and 3.9, it is seen that the carbide catalysts behave in a similar manner toward S-heterocycles, and that they are more selective

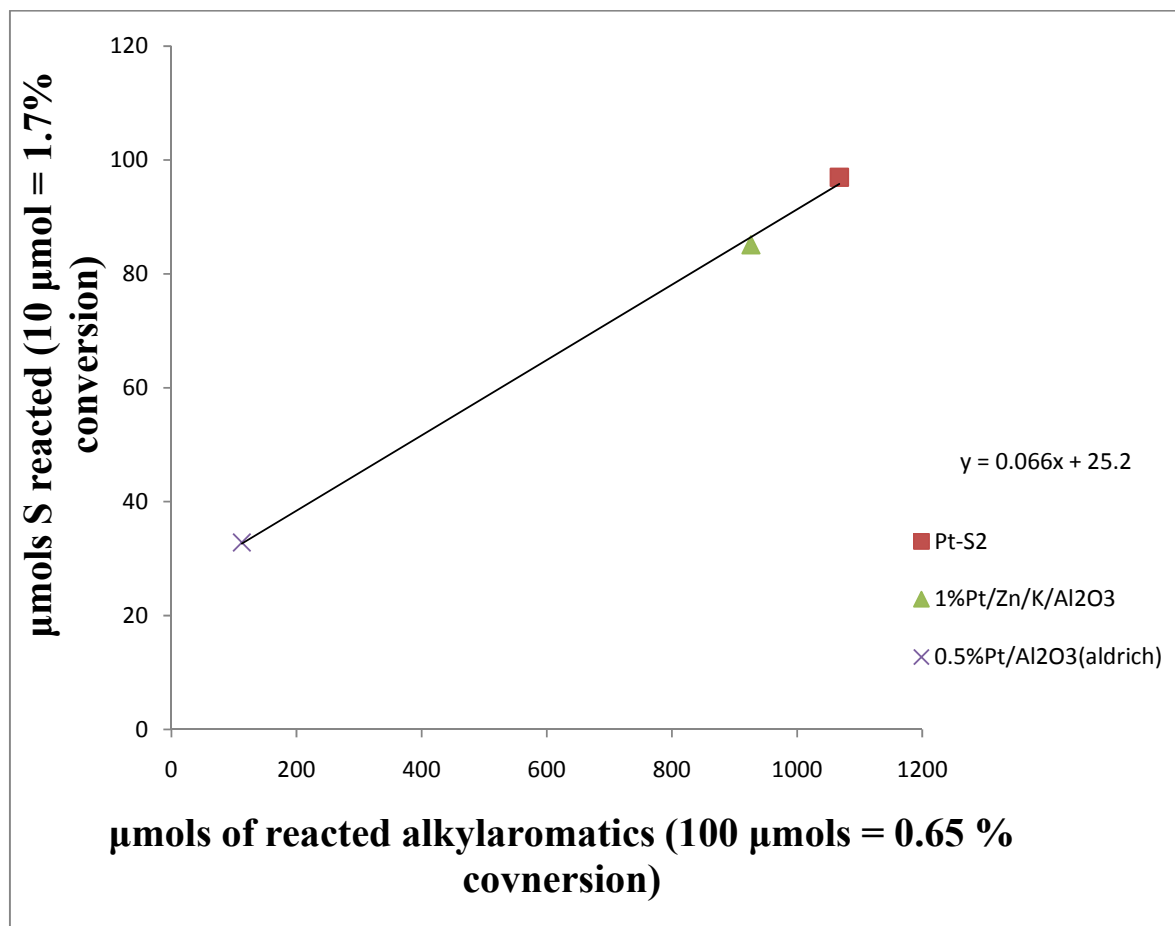


Figure 3.7 Selectivity of Pt group catalysts for S-heterocycles

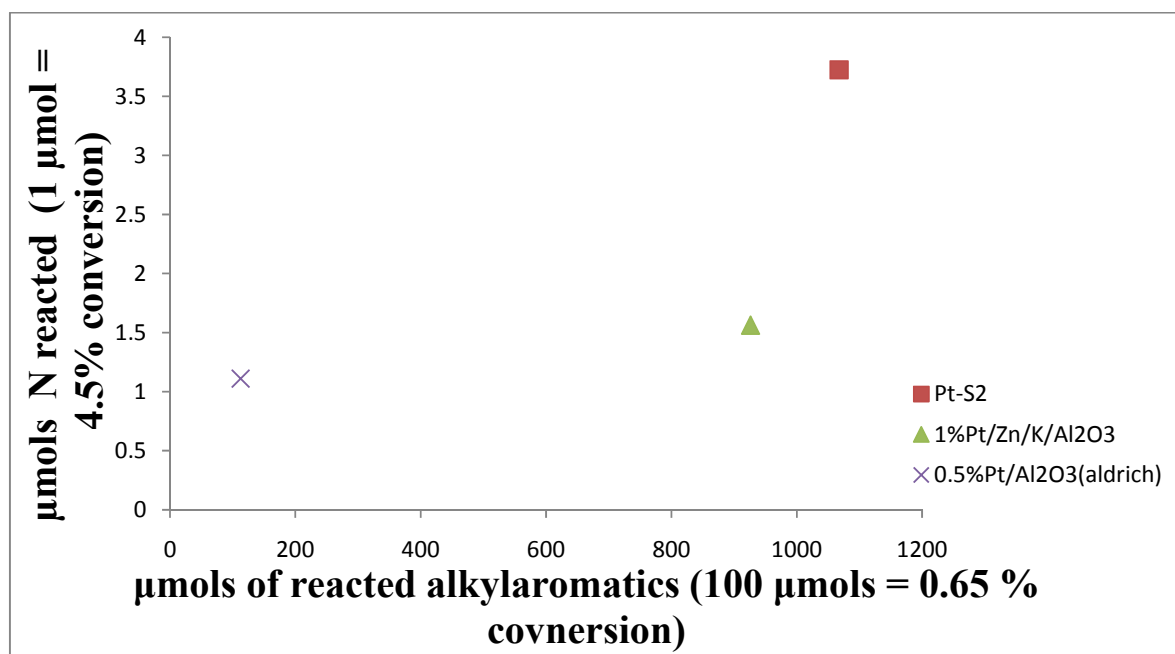


Figure 3.8 Selectivity of Pt group catalysts for N-heterocycles

than the base metal catalysts (compare Fig. 3.8 to 3.3). The Mo₂C supported on the HNO₃-pretreated activated carbon (CDX2) was more active for either S-heterocycle or N-heterocycle oxidation, although they are poorly selective for the latter. A higher reaction pressure led to a decrease in the amount of reacted alkylaromatics, S-heterocycles and N-heterocycles, but this is based on very limited data. There was a general increase in the oxidation of N-heterocycles vs. alkylaromatics.

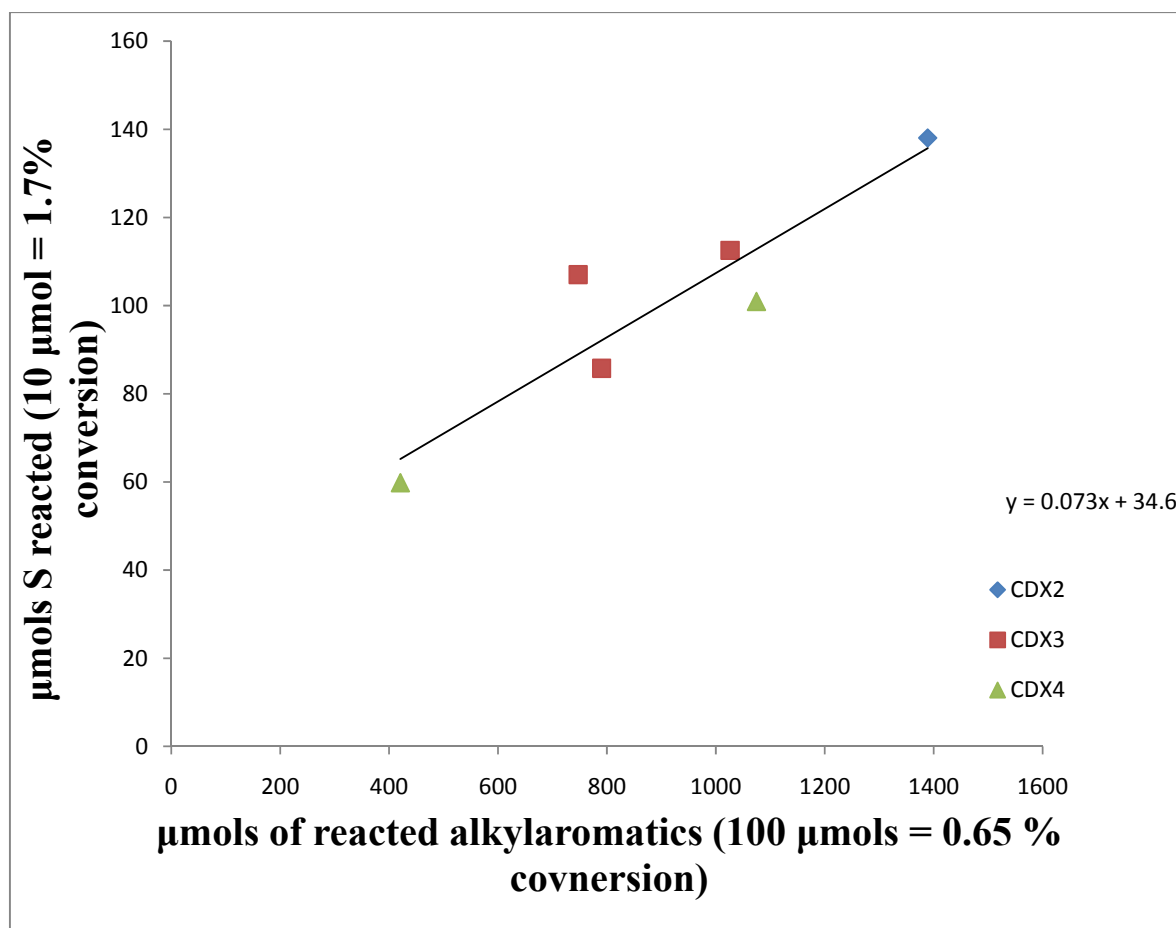


Figure 3.9 Selectivity of Carbide group catalysts for S-heterocycles

3.3.5 Pd Catalysts

For Pd/Al₂O₃ catalysts, different loading catalysts (0.5%, 4% nominal loading) were tested at 343 and 363K, and 0.791, 1.14 and 1.83 MPa. One run's results (OD60 was

discarded because it showed high conversions of ethylbenzene and thiophene were not repeated using either CDX6 or any other catalyst. As expected, the higher loading catalysts

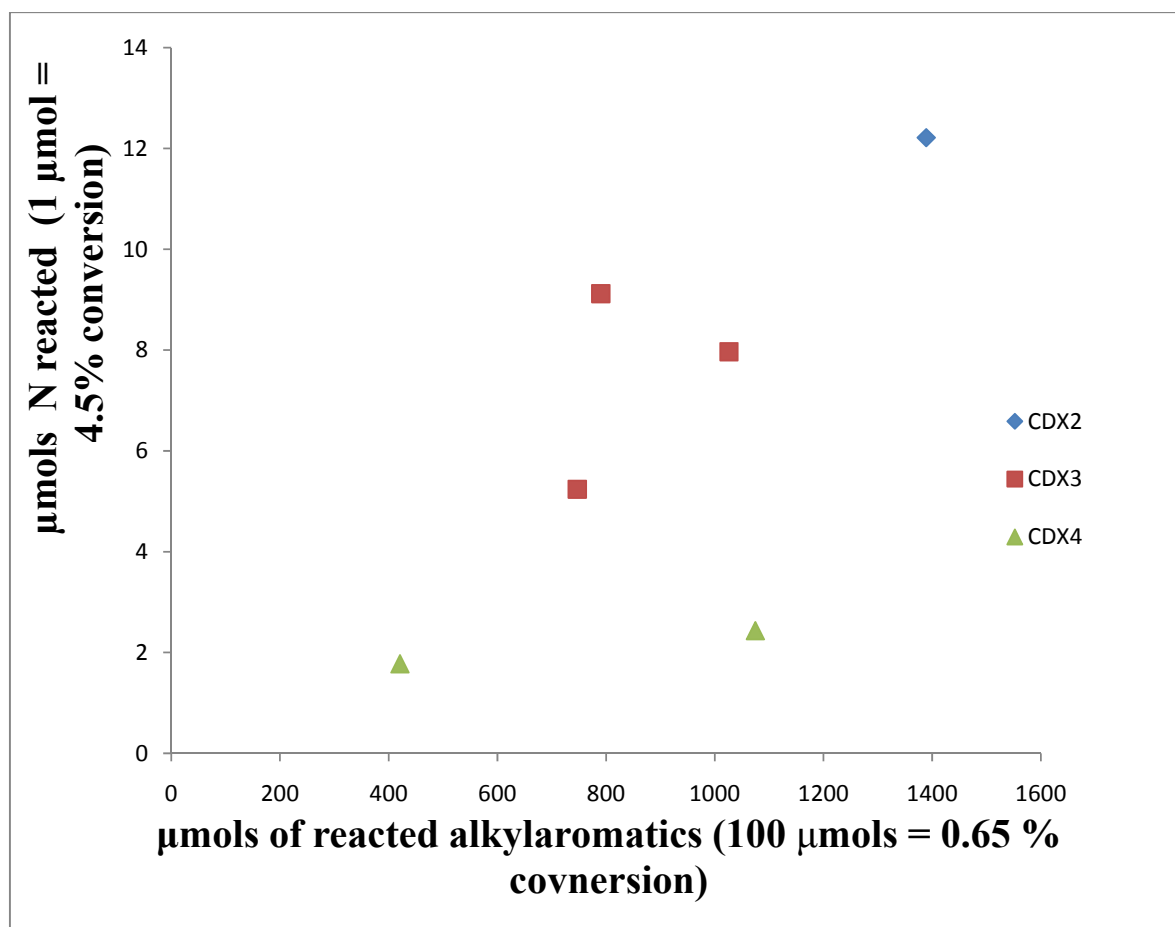


Figure 3.10 Selectivity of carbide group catalysts for N-heterocycles

(CDX5 and CDX6) are more active. The Pd/Al₂O₃ catalysts are similar in S-heterocycle selectivity to the base metal catalysts but less selective than the carbides (compare Figs. 3.11 and 3.9). They are similar to the base metals in terms of activity for N-heterocycle oxidation (compare Figs. 3.12 and 3.4). The difference in the Pd dispersion between CDX6 (9%) and CDX5 (56%) probably led to their different activities for S-heterocycle oxidation.

The Pd/C catalysts were examined more closely because they are commercial materials (in contrast to the metal carbides), and they showed initial promise. Several combinations of temperature (343, 363K), pressure (0.58, 0.79, 1.14, 1.83 MPa), catalysts (5% Pd/MPT-5, 5%

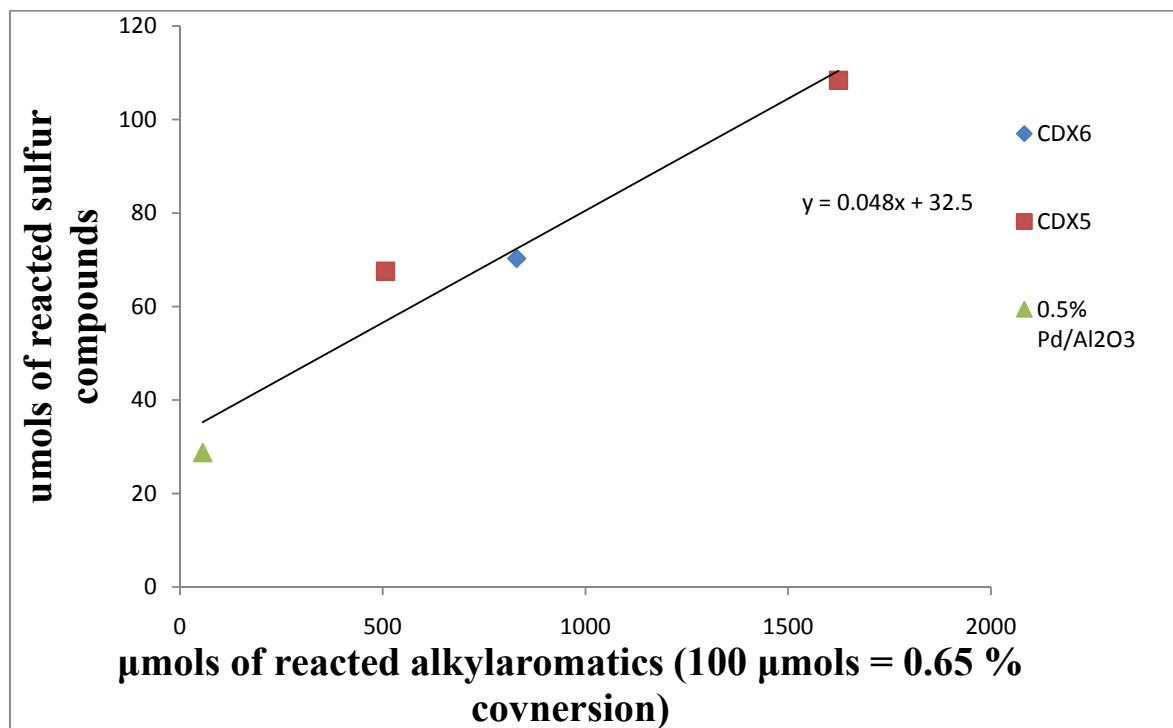


Figure 3.11 Selectivity of Pd/Al₂O₃ catalysts for S-heterocycles

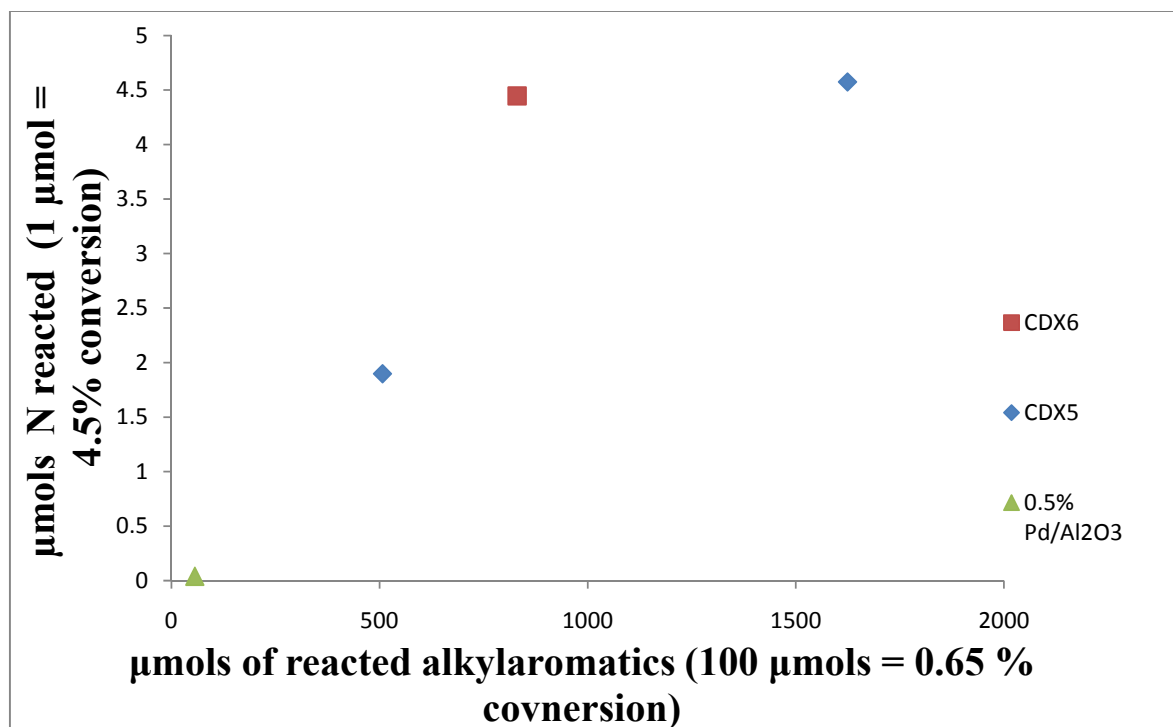


Figure 3.12 Selectivity of Pd/Al₂O₃ catalysts for N-heterocycles

Pd/Deg and 5% Pd/Eng) and reaction times (2, 3, 4 h) were examined in order to find the optimal catalyst and reaction conditions. Using Figs. 3.13 and 3.14, it is unclear at this point if the behavior is uniform or not for these catalysts. More data are probably necessary for all of the catalysts. Therefore the catalysts were not grouped together in the Figures. The 5% Pd/Eng showed a lower activity for both S-heterocycles and N-heterocycles, while the 5% Pd/MPT-5 was the most active and most selective for S-heterocycle oxidation. The activity of 5% Pd/Deg was intermediate. There was no trend in the oxidation of the N-heterocycles vs. alkylaromatics.

From Table 3.6, it is seen that an increase in reaction temperature and pressure both lead to an increase in the amount of reacted alkylaromatics. The activity of 5% Pd/MPT-5 toward S-heterocycles increased with temperature. At 343K, the amounts of reacted S-heterocycles at various O₂ pressures were: 106 μmol (1.14 MPa); 89 (1.83 MPa) > 44 (0.79 MPa). So the optimal O₂ pressure at 343K is > 1 MPa.

The better S-heterocycle activity and selectivity of Pd/MPT-5 may be related to lower basicity of the support. The contact pH of 5%Pd/MPT-5 was 6.99, that of 5%Pd/Deg 8.21, and that of 5%Pd/Eng (least active) 9.31. The S-heterocycles are weak bases (nucleophiles) themselves, so this might be interpreted as an S-heterocycle binding phenomenon. There may have been a stronger adsorption on the more neutral carbon, leading to more S-heterocycles in the vicinity of Pd sites. Note that the MPT-5 carbon is neither the highest in surface area or dispersion, nor is it an "eggshell" catalyst such as 5%Pd/Deg (where more of the Pd is located nearer to the external surfaces of the particles). So as its superior performance cannot be explained by any of these more conventional reasons, it must have something to do with the nature of the carbon itself.

Table 3.6 Reaction conditions for experiments using 5% Pd/MPT-5

Catalyst	$N_S^{R^1}$ (μmol)	$N_N^{R^2}$ (μmol)	$N_A^{R^3}$ (μmol)	T (K)	P (MPa)	Time (h)
5% Pd/C MPT-5	38	3.5	280	343	0.58	2
	31	5.1	120	343	0.58	2
	44	7.9	180	343	0.79	4
	69	6.4	330	363	0.79	4
	89	6.6	950	343	1.83	4
	110	9.0	830	343	1.14	4

¹ Reacted N-heterocycles

² Reacted S-heterocycles

³ Reacted alkylaromatics

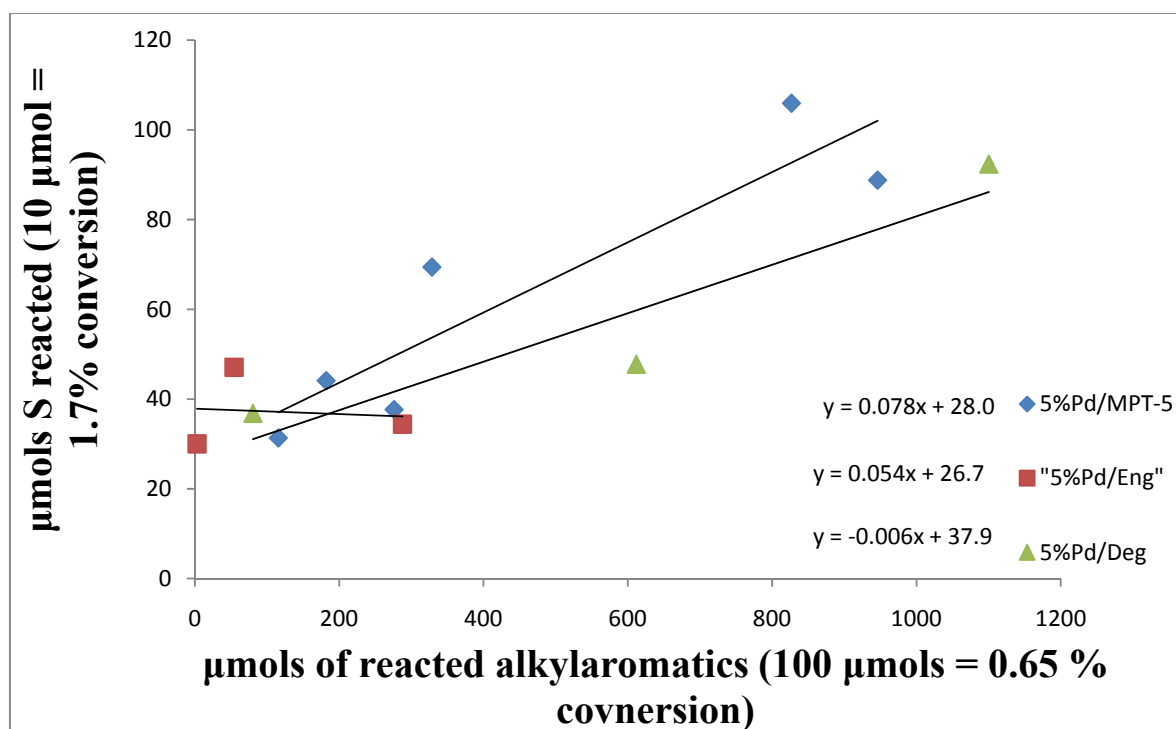


Figure 3.13 Selectivity of Pd/Carbon group catalysts for S-heterocycles

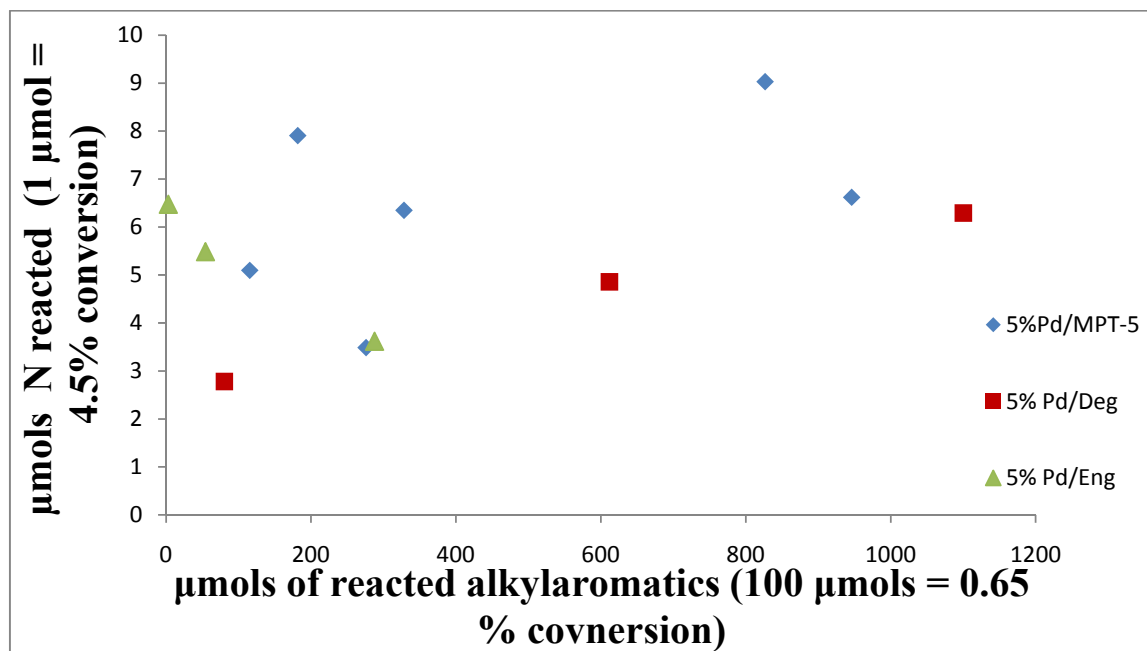


Figure 3.14 Selectivity of Pd/Carbon group catalysts for N-heterocycles

CHAPTER 4 SUMMARY AND CONCLUSION

ODS using O₂ with several groups of catalysts (base metal, heteropolyacid, carbide, supported Pt, Pd/C and Pd/Al₂O₃ catalysts) was studied in this research project. The reaction conditions (343-363 K and 0.8 – 1.8 MPa of O₂) are milder than in the HDS process (usually ~623 K and 3 MPa of H₂).⁷⁸ In addition to advantages of low costs associated with mild reaction conditions, the ODS process using O₂ avoids the danger in handling organo-peroxides or hydrogen peroxide. The parallel catalytic oxidations of alkylaromatics and N-heterocycles were also investigated, in contrast to most other research in ODS, and in contrast to all other ODS work using O₂. Although some researchers have reported higher reaction rates of S-heterocycles, their reaction temperatures (473-573 K) are much higher than used here. The higher reaction temperatures in ODS are undesirable if the selectivity of S-heterocycle oxidation over alkylaromatics oxidation is considered.

An optimal catalyst for the ODS reaction requires not only activity but also selectivity for the oxidation of S-heterocycles and N-heterocycles. The selectivity can be demonstrated by the slope and intercept of the regression lines in the selectivity plots. The activity can be represented by the maximum conversions of S-heterocycles and N-heterocycles.

The maximum conversion of S-heterocycles is calculated as follows:

$$X_S^* = 1 - \frac{C_{\text{Thiophene}}^0 \times X_{\text{Thiophene}} + C_{\text{DBT}}^0 \times X_{\text{DBT}}}{C_{\text{Thiophene}}^0 + C_{\text{DBT}}^0}$$

The maximum conversion of N-heterocycles is calculated as follows:

$$X_N^* = 1 - \frac{C_{\text{Acridine}}^0 \times X_{\text{Acridine}} + C_{\text{Carbazole}}^0 \times X_{\text{Carbazole}}}{C_{\text{Acridine}}^0 + C_{\text{Carbazole}}^0}$$

The maximum conversion of alkylaromatics is calculated as follows:

$$X_A^* = 1 - \frac{C_{\text{Ethylbenzene}}^0 \times X_{\text{Ethylbenzene}} + C_{\text{1-Methylnaphthalene}}^0 \times X_{\text{1-Methylnaphthalene}}}{C_{\text{Ethylbenzene}}^0 + C_{\text{1-Methylnaphthalene}}^0}$$

I will review the performance of each class of catalysts (e.g. base metal, heteropolyacid, carbide, supported Pt, Pd/C and Pd/Al₂O₃ catalysts). For Pd/C catalysts, I found that

5%Pd/MPT-5 was the best ODS catalyst. The slopes and intercepts of the best of each class of catalyst are summarized in Tables 4.1 and 4.2. For S-heterocycle oxidation, the top three classes are Pd/C, supported Mo₂C and the supported Pt catalysts. This judgment is based on the combination of heterocycle maximum conversion, high intercept, high slope, and low alkylaromatic conversion. For N-heterocycle oxidation, the top three classes are Pd/C, supported Mo₂C and Pd/Al₂O₃. This judgment is based on maximum heterocycle conversion and low alkylaromatic conversion.

The optimal conditions for S-heterocycle selectivity for 5% Pd/MPT-5 and the supported Mo₂C are at around 343K, 1 MPa O₂.

.Table 4.1 Summary of optimal catalysts for S-heterocycles.

Catalyst	Slope for S/Alkylaromatics	Intercept for S/Alkylaromatics	X _S *	X _A *
5% Pd/C	0.078	28	18%	5%
Carbide	0.073	39	23%	9%
Pd/Al ₂ O ₃	0.048	32	18 %	11%
Heteropolyacid	0.026	17	5%	0%
Base Metal	0.052	24	16%	10%
Pt Group	0.066	25	15%	6%

The behavior of the base metal catalysts (CoSi1 and ReSi1) and the heteropolyacid catalyst (CsHPW-SiO₂) showed there could be two different types of active sites (active for S-heterocycles and N-heterocycles respectively) on the surfaces of these catalysts. The active site for N-heterocycles on these catalysts can be poisoned by the products of alkylaromatics oxidations.

Table 4.2 Summary of optimal catalysts for N-heterocycles.

Catalyst	X_N^*	X_A^*
5% Pd/C	41%	5%
Carbide	55%	9%
Pd/Al ₂ O ₃	21%	11%
Heteropolyacid	5%	0%
Base Metal	21%	10%
Pt Group	7 %	6%

Based on the analysis of the oxidation products, it can be concluded that the sulfones expected from the oxidation of DBT and thiophene remained adsorbed on the surfaces of the catalysts. This phenomenon has also been reported in literature.⁶⁶ Second, the air oxidation of ethylbenzene and 1-methylnaphthalene gave products that can generate organo-peroxides, and these compounds could be causing further oxidation of N-heterocycles and S-heterocycles.

The optimal ODS catalysts (Mo₂C/C and 5% Pd/MPT-5) also showed high activity (as high as 50% conversion) for N-heterocycles. This characteristic is very different from the commercial HDS catalysts (supported CoMoS), which can be poisoned by N-heterocycles.⁷⁹ The activity of HDS catalysts is also decreased by organic heterocompounds and polyaromatic hydrocarbons,⁷⁹ for which the following order of inhibition has been reported: saturated and monoaromatic hydrocarbons < condensed aromatics ≈ oxygen compounds ≈ hydrogen sulfide < organic sulfur compounds < basic nitrogen compounds.⁸⁰ Ease of removal of N-heterocycles by ODS could be beneficial for the catalysts used in HDS, if the ODS process could be combined with a conventional HDS process. The ODS process would remove the N-heterocycles, DBT, and alkylated DBTs, while the HDS process would remove

the sulfides and thiophenes that are sometimes more resistant to ODS. Because of the increased interest in processing shale oil and oil sands, it will become more important to remove heavy N-heterocycles which are present in these feeds. The ODS process show good prospects for the above application.

There are at least three reports on using O₂ to directly oxidize sulfur compounds in actual or synthetic fuel.^{10,11,7} Sampanthar et. al. reported that MnO₂ and Co₂O₃ supported on γ -Al₂O₃ can catalyze the air oxidation of S-heterocycles in real diesel at 403-473 K.¹⁰ After 24 h of reaction, 60% of 4-methyl-DBT, 4,6-dimethyl-DBT and 4,6-diethyl-DBT disappeared at 453 K, while the content of aromatics in the diesel dropped from 46.4% to 12.5%. Although the conversion of S-heterocycles was high (60%), the conversion of aromatics was also high (73%). This is harmful to the quality of the diesel. Also the S-heterocycles used in this work were mainly methyl substituted DBTs, in which the electron density at the S atom is higher than for DBT and thiophene. As discussed in the Chapter 1, increased electron density makes S-heterocycles more reactive toward oxidation. Song et. al.⁷ reported that an Fe(NO₃)₃-FeBr₃/AC catalyst is active in catalyzing the O₂ oxidation of DBT, benzothiophene and 2-methyl-BT at 298 K. The conversion of S-heterocycles in JP-8 fuel was 38% after 2 h. There was no investigation into catalytic oxidation of N-heterocycles or alkylaromatics. Lu et. al.¹¹ reported the 95% of the S-heterocycles (thiophene and BT) in isooctane can be converted into SO₂ by air at 573 K using Cu/CeO₂ and Pt/CeO₂. The catalytic oxidation of the N-heterocycles and alkylaromatics was not reported. And the reaction temperature was much higher compared with that used here. Compared to previous work on ODS with O₂, this work shows that Mo₂C/C and 5% Pd/C catalysts can oxidize S-heterocycles at milder conditions where alkylaromatic oxidation is less of a problem, and with reasonable activity for converting N-heterocycles.

REFERENCES

- ¹ US EPA, Regulatory Announcement: Heavy-Duty Engine and Vehicle Standards and Highway Fuel Sulfur Control Requirements, December, 2000.
- ² C. S. Song and X. L. Ma. New design approaches to ultra-clean diesel fuels by deep desulfurization and deep dearomatization. *Applied Catalysis B: Environmental* **2003**, 41, 207-238.
- ³ J. M. Thomas and W. J. Thomas. Principles and practice of heterogeneous catalysis, VCH 1997, 638.
- ⁴ C. S. Song. An overview of new approaches to deep desulfurization for ultra-clean gasoline, diesel fuel and jet fuel. *Catalysis Today* **2003**, 86(1-4), 211-263.
- ⁵ J. A. Babich and J. A. Moulijn. Science and technology of novel processes for deep desulfurization of oil refinery streams: a review. *Fuel* **2003**, 82, 607-631.
- ⁶ A. Attar and W. H. Corcoran. Desulfurization of organic sulfur compounds by selective oxidation. 1. Regenerable and nonregenerable oxygen carriers. *Industrial & Engineering Chemistry Product Research and Development* **1978**, 17 (2), 102.
- ⁷ X. L. Ma, A. N. Zhou and C. S. Song. A novel method for oxidative desulfurization of liquid hydrocarbon fuels based on catalytic oxidation using molecular oxygen coupled with selective adsorption. *Catalysis Today* **2007**, 123, 276-284.
- ⁸ R. G. Leliveld and S. E. Eijssbouts. How a 70-year-old catalytic refinery process is still everdependent on innovation. *Catalysis Today* **2008**, 130, 183-189.
- ⁹ H. Topsøe. Developments in operando studies and in situ characterization of heterogeneous catalysts. *Journal of Catalysis* **2003**, 216, 155-164.
- ¹⁰ J. T. Sampanthar, H. Xiao, J. Dou, T. Y. Nah, X. Rong and W. P. Kwan. A novel oxidative desulfurization process to remove refractory sulfur compounds from diesel fuel. *Applied Catalysis B: Environmental* **2006**, 63, 85-93.
- ¹¹ Y. Lu, Y. Wang, L. Gao, J. Chen, J. Mao, Q. Xue, Y. Liu, H. Wu, G. Gao and M. He. Aerobic oxidative desulfurization: A promising approach for sulfur removal from fuels. *ChemSusChem* **2008**, 1, 302 -306.
- ¹² S. Murata, K. Murata, K. Kidena and M. Nomura. A novel oxidative desulfurization system for diesel fuels with molecular oxygen in the presence of cobalt catalyst and aldehydes. *Energy & Fuels* **2004**, 18, 116-121.

- ¹³ S. Otsuki, T. Nonaka, N. Takashima, W. Qian, A. Ishihara, T. Imai and T. Kabe. Oxidative desulfurization of light gas oil and vacuum gas oil by oxidation and solvent extraction. *Energy Fuels* **2000**, 14 (6), 1232-1239.
- ¹⁴ M. Te, C. Fairbridge and Z. Ring. Oxidation reactivities of dibenzothiophenes in polyoxometalate/H₂O₂ and formic acid/H₂O₂ systems. *Applied Catalysis A: General* **2001**, 219, 267-280.
- ¹⁵ V. Dumont, L. Oliviero, F. Maugé and M. Houalla. Oxidation of dibenzothiophene by a metal–oxygen–aldehyde system. *Catalysis Today* **2008**, 130, 195-198.
- ¹⁶ D. Zhao, H. Ren, J. Wang, Y. Yang and Y. Zhao. Kinetics and mechanism of quaternary ammonium salts as phase transfer catalysts in the liquid-liquid phase for oxidation of thiophene. *Energy & Fuels* **2007**, 21, 2543-2547.
- ¹⁷ L. C. Caero, E. Hernández, F. Pedraza and F. Murrieta. Oxidative desulfurization of synthetic diesel using supported catalysts. Part 1. Study of the operation conditions with a vanadium oxide based catalyst. *Catalysis Today* **2005**, 107-108, 564-569.
- ¹⁸ L. C. Caero, F. Jorge, A. Navarro and A. Gutiérrez-Alejandre. Oxidative desulfurization of synthetic diesel using supported catalysts. Part 1. Effect of oxidant and nitrogen compound on extraction-oxidation process. *Catalysis Today* **2006**, 116, 562-568.
- ¹⁹ F. A. Shahrani, T. Xiao, S. A. Llewellyn, S. Barri, Z. Jiang, H. Shia, G. Martinie and M. L.H. Green. Desulfurization of diesel via the H₂O₂ oxidation of aromaticsulfides to sulfones using a tungstate catalyst. *Applied Catalysis B: Environmental* **2007**, 73, 311-316.
- ²⁰ Y. Wang, G. Li, X. Wang and C. Jin. Oxidative desulfurization of 4,6-dimethyldibenzothiophene with hydrogen peroxide over Ti-HMS. *Energy & Fuels* **2007**, 21, 1415-1419.
- ²¹ Y. Shiraishi, T. Naito and T. Hirai. Vanadosilicate molecular sieve as a catalyst for oxidative desulfurization of light oil. *Industrial & Engineering Chemistry Research* **2003**, 42, 6034-6039.
- ²² Y. Fang and H. Hu. Mesoporous TS-1: Nanocasting synthesis with CMK-3 as template and its performance in catalytic oxidation of aromatic thiophene. *Catalysis Communication* **2007**, 8, 817-820.
- ²³ K. Yazu, Y. Yamamoto, T. Furuya, K. Miki and K. Ukegawa. Oxidation of dibenzothiophenes in an organic biphasic system and its application to oxidative desulfurization of light oil. *Energy & Fuels* **2001**, 15, 1535-1536.
- ²⁴ J. Palomeque, J. M. Clacens and F. Figueras. Oxidation of dibenzothiophen by hydrogen peroxide catalyzed by solid bases. *Journal of Catalysis* **2002**, 211, 103-108.

- ²⁵ V. Hulea, A. L. Maciuca, F. Fajula and E. Dumitriu. Catalytic oxidation of thiophenes and thioethers with hydrogen peroxide in the presence of W-containing layered double hydroxides. *Applied Catalysis A: General* **2006**, 313, 200-207.
- ²⁶ A. Deshpande, A. Bassi and A. Prakash. Ultrasound-assisted, base-catalyzed oxidation of 4,6- Dimethyldibenzothiophene in a biphasic diesel-acetonitrile system. *Energy & Fuels* **2005**, 19, 28-34.
- ²⁷ L. F. Ramirez-Verduzco, J. A. DelosReyes and E. Torres-Garcia. Solvent effect in homogenous and heterogenous reactions to remove dibenzothiophenes by an oxidation and extraction Scheme. *Industrial & Engineering Chemistry Research* **2008**, 47(15), 5353-5361.
- ²⁸ J. L. García-Gutiérrez, G. A. Fuentes, M. E. Hernández-Terán, F. Murrieta, J. Navarrete and F. Jiménez-Cruz. Ultra-deep oxidative desulfurization of diesel fuel with H₂O₂ catalyzed under mild conditions by polymolybdates supported on Al₂O₃. *Applied Catalysis A: General* **2006**, 305, 15-20.
- ²⁹ F. Mashio, S. Kato. *Yuki Gousei Kagaku* **1968**, 26, 367.
- ³⁰ D.Wang, E.W. Qian, H. Amano, K. Okata, A. Ishihara and T. Kabe. Oxidative desulfurization of fuel oil: Part I. Oxidation of dibenzothiophenes using tert-butyl hydroperoxide. *Applied Catalysis A: General* **2003**, 253, 91-99.
- ³¹ G. Yu, S. Lu, H. Chen, and Z. Zhu. Oxidative desulfurization of diesel fuels with hydrogen peroxide in the presence of activated carbon and formic acid. *Energy & Fuels* **2005**, 19, 447-452.
- ³² X. Si, S. Cheng, Y. Lu, G. Gao and M. Y. He. Oxidative desulfurization of model oil over Au/Ti-MWW. *Catalysis Letters* **2008**, 122, 321-324.
- ³³ B. Zapata, F. Pedraza and M. A. Valenzuela. Catalyst screening for oxidative desulfurization using hydrogen peroxide. *Catalysis Today* **2005**, 106, 219-221.
- ³⁴ D. Huang, Y. J. Wang, L. M. Yang, and G. S. Luo. Chemical oxidation of dibenzothiophene with a directly combined amphiphilic catalyst for deep desulfurization. *Industrial & Engineering Chemistry Research* **2006**, 45, 1880-1885.
- ³⁵ K. J. Stanger and R. J. Angelici. Silica-catalyzed tert-butyl hydroperoxide oxidation of dibenzothiophene and its 4,6-dimethyl derivative: A route to low-sulfur petroleum feedstocks. *Energy & Fuels* **2006**, 20, 1757-1760.
- ³⁶ V.V.D.N. Prasad, K. E. Jeong, H. J. Chae, C. U. Kim and S. Y. Jeong. Oxidative desulfurization of 4,6-dimethyl dibenzothiophene and light cycle oil over supported molybdenum oxide catalysts. *Catalysis Communications* **2008**, 9, 1966-1969.

- ³⁷ A. Chica, A. Corma and M. E. Domine. Catalytic oxidative desulfurization (ODS) of diesel fuel on a continuous fixed-bed reactor. *Journal of Catalysis* **2006**, 242, 299-308.
- ³⁸ A. Angelis, P. Pollesel, D. Molinari, W. O. Parker, A. Frattini, F. Cavani, S. Martins and C. Perego. Heteropolyacids as effective catalysts to obtain zero sulfur diesel. *Pure and Applied Chemistry* **2007**, 79(11), 1887-1894.
- ³⁹ K. J. Stanger, J. W. Wiench, M. Pruski, J. H. Espenson, G. A. Kraus and R. J. Angelici. Catalytic oxidation of a thioether and dibenzothiophenes using an oxorhenium(V) dithiolate complex tethered on silica. *Journal of Molecular Catalysis A: Chemical* **2006**, 243, 158-169.
- ⁴⁰ A. Ishihara, D. Wang, F. Dumeignil, H. Amano, E. W. Qian and T. Kabe. Oxidative desulfurization and denitrogenation of a light gas oil. *Applied Catalysis A: General* **2005**, 279, 279-287.
- ⁴¹ R. A. Sheldon. Synthetic and mechanistic aspects of metal-catalysed epoxidations with hydroperoxides. *Journal of Molecular Catalysis* **1980**, 7, 107-126.
- ⁴² C. G. Overberger and R. W. Cummins. Mechanism of the oxidation of p,p'-dichlorobenzyl sulfide by deroxybenzoic and para substituted deroxybenzoic acids. *Journal of the American Chemical Society* **1953**, 75, 4250-4254.
- ⁴³ L. Bateman and K. R. Hargrave. Oxidation of organic sulphides. I. Interaction of cyclohexyl methyl sulphide with hydroperoxides in alcohols. *Proceedings of the Royal Society A* **1954**, 224, 389-398.
- ⁴⁴ P. D. Filippis and M. Scarcellar. Functionalized hexagonal mesoporous silica as an oxidizing agent for the oxidative desulfurization of organosulfur compounds. *Industrial & Engineering Chemistry Research* **2008**, 47, 973-975.
- ⁴⁵ P. D. Costa, C. Potvin, J.M. Manoli, M. Breysse and G. D. Mariadassou. Novel phosphorus-doped alumina-supported molybdenum and tungsten carbides: synthesis, characterization and hydrogenation properties. *Catalysis Letters* **2001**, 72(1-2), 91-97.
- ⁴⁶ D. Mordenti, D. Brodzki and G. D. Mariadassou. New synthesis of Mo₂C 14nm in average size supported on a high specific surface area carbon material. *Journal of Solid State Chemistry* **1998**, 141(1), 114-120.
- ⁴⁷ L. Salvati, L. E. Makovsky, J. M. Stencel, F. R. Brown and D. M. Hercules. Surface spectroscopic study of tungsten-alumina catalysts using X-ray photoelectron, ion scattering, and Raman spectroscopies. *The Journal of Physical Chemistry* **1981**, 85, 3700-3707.
- ⁴⁸ V. N. M. Rao, F. J. Weigert and L. E. Manzer. Catalytic process for producing CCl₃CF₃. US Patent 5,120,883, 1992.

- ⁴⁹ P. S. Furmanek, D. A. Glasscock, M. J. Keane, B. A. Mahler and V. N. M. Rao. Production of dihalomethanes containing fluorine and azeotropes of dihalomethanes containing chlorine with HF. World Patent, 1995, 012563.
- ⁵⁰ V.N.M. Rao and F.J. Weigert. Catalytic process for producing CCl_3CF_3 , WO/1993/004024.
- ⁵¹ P. D. Costa, J. L. Lemberon, C. Potvin, J. M. Manoli, G. Perot, M. Breysse and G. D. Mariadassou. Tetralin hydrogenation catalyzed by $\text{Mo}_2\text{C}/\text{Al}_2\text{O}_3$ and $\text{WC}/\text{Al}_2\text{O}_3$ in the presence of H_2S . *Catalysis Today* **2001**, 65, 195-200.
- ⁵² R. J. Farrauto, J. K. Lampert, M. C. Hobson and E. M. Waterman. Thermal decomposition and reformation of PdO catalysts; support effects. *Applied Catalysis B: Environmental* **1995**, 6(3), 263-270.
- ⁵³ M. V. Rahaman and M.A. Vannice. The hydrogenation of toluene and *o*-, *m*-, and *p*-xylene over palladium: I. Kinetic behavior and *o*-xylene isomerization. *Journal of Catalysis* **1991**, 127(1), 251-266.
- ⁵⁴ X. Wang, C. Liang and S. Dai. Facile synthesis of ordered mesoporous carbons with high thermal stability by self-assembly of resorcinol- formaldehyde and block copolymers under highly acidic conditions. *Langmuir* **2008**, 24, 7500-7505.
- ⁵⁵ A. L. Dantas Ramos, P. da Silva Alves, D. A. G. Aranda and M. Schmal. Characterization of carbon supported palladium catalysts: inference of electronic and particle size effects using reaction probes. *Applied Catalysis A: General* **2004**, 277, 71-81.
- ⁵⁶ M. L. Toebes, J. A. van Dillen and K. P. de Jong. Synthesis of supported palladium catalysts. *Journal of Molecular Catalysis A: Chemical* **2001**, 173(1-2), 75-98.
- ⁵⁷ R. Ryoo, S. H. Joo and S. Jun. Synthesis of highly ordered carbon molecular sieves via template-mediated structural transformation. *The Journal of Physical Chemistry B* **1999**, 103, 7743-7746.
- ⁵⁸ R. Ryoo, S.H. Joo, M. Kruk and M. Jaroniec. Ordered mesoporous carbons. *Advanced Materials* **2001**, 13, 677-680.
- ⁵⁹ B. Sakintuna and Y. Yurum. Templated porous carbons: a review article. *Industrial & Engineering Chemistry Research* **2005**, 44, 2893-2902.
- ⁶⁰ E. Garcia-Bordeje, F. Kapteijn and J. A. Moulijn. Preparation and characterization of carbon-coated monoliths for catalyst supports. *Carbon* **2002**, 40, 1079-1088.

- ⁶¹ H. Markus, P. Mäki-Arvela, N. Kumar, N. V. Kul'kova, P. Eklund, R. Sjöholm, B. Holmbom, T. Salmi and D.Y. Murzin. Hydrogenolysis of hydroxymatairesinol over carbon-supported palladium catalysts. *Catalysis Letters* **2005**, 103(1–2), 125-131.
- ⁶² M. L. Toebes, J.A. van Dillen and K.P. de Jong. Synthesis of supported palladium catalysts. *Journal of Molecular Catalysis A: Chemical* **2001**, 173, 75-98.
- ⁶³ B. N. Heimlich and T. J. Wallace. Kinetics and mechanisms of the oxidation of dibenzothiophene in hydrocarbon solution. *Tetrahedron* **1966**, 22, 3571-3579.
- ⁶⁴ S. S. Barton, M. J. B. Evans, E. Halliop and J. A. F. Macdonald. Acidic and basic sites on the surface of porous carbon. *Carbon* **1997**, 35, 1361-1366.
- ⁶⁵ R. S. Drago, B. Wayland and R. L. Carlson. Donor properties of sulfoxides, alkyl sulfites, and sulfones. *Journal of the American Chemical Society* **1963**, 85, 3125-3128.
- ⁶⁶ J. T. Miller, K. P. Keckler, J. L. Yedinak and R. R. Simpson. Oxidative desulfurization process. US patents: 208249.
- ⁶⁷ J. H. Kim, X. Ma, A. Zhou and C. S. Song. Ultra-deep desulfurization and denitrogenation of diesel fuel by selective adsorption over three different adsorbents: A study on adsorptive selectivity and mechanism. *Catalysis Today* **2006**, 111(1-2), 74-83.
- ⁶⁸ P.P. Toribio¹, J.M. Campos-Martin and J.L.G. Fierro. Liquid-phase ethylbenzene oxidation to hydroperoxide with barium catalysts. *Journal of Molecular Catalysis A: Chemical* **2005**, 227, 101-105.
- ⁶⁹ K. J. Stanger and R. J. Angelici. Silica-catalyzed *tert*-butyl hydroperoxide oxidation of dibenzothiophene and its 4,6-dimethyl derivative: a route to low-sulfur petroleum feedstocks. *Energy & Fuels* **2006**, 20, 1757-1760.
- ⁷⁰ J. M. Aubry, C. Pierlot, J. Rigaudy And R. Schimidt. Reversible binding of oxygen to aromatic compounds. *Accounts of Chemical Research* **2003**, 36, 668-675.
- ⁷¹ K. Yasukouchi, I. Tanicuchi, H. Yamaguchi and K. Arakawa. Anodic oxidation of acridine in acetonitrile. *Journal of Electroanalytical Chemistry* **1981**, 121, 231-240.
- ⁷² Y. Shiraishi, T. Hirai and I. Komasaawa. Oxidative desulfurization process for light oil using titanium silicate molecular sieve catalysts. *Journal of Chemical Engineering of Japan* **2002**, 35(12), 1305-1311.
- ⁷³ S. M. Resnick, D. S. Torok and D. T. Gibson. Oxidation of carbazole to 3-hydroxycarbazole by naphthalene 1,2-dioxygenase and biphenyl 2,3-dioxygenase. *FEMS Microbiology Letters* **2006**, 113(3), 297- 302.

- ⁷⁴ H. Nojiri, J. W. Nam, M. Kosaka, K. I. Morii, T. Takemura, K. Furihata, H. Yamane and T. Omori. Diverse oxygenations catalyzed by carbazole 1,9-dioxygenase from *Pseudomonas* sp. strain ca10. *Journal of Bacteriology* **1999**, 181(10), 3105-3113.
- ⁷⁵ H. Taoudi, J. C. Bernede, A. Bonnet, M. Morsli and A. Godoy. Comparison of polycarbazole obtained by oxidation of carbazole either in solution or in thin film form. *Thin Solid Films* **1997**, 304(1-2), 48-55.
- ⁷⁶ Y. Shiraishi, T. Naito and T. Hirai. Vanadosilicate molecular sieve as a catalyst for oxidative desulfurization of light oil. *Industrial and Engineering Chemistry Research* **2003**, 42(24), 6034-6039.
- ⁷⁷ S. Fujibayashi, K. Nakayama, M. Hamamoto, S. Sakaguchi, Y. Nishiyama and Y. Ishii. An efficient aerobic oxidation of various organic compounds catalyzed by mixed addenda heteropolyoxometalates containing molybdenum and vanadium. *Journal of Molecular Catalysis A: Chemical* **1996**, 110, 105-117.
- ⁷⁸ P. Grange, X. Vanhaeren. Hydrotreating catalysts, an old story with new challenges. *Catalysis Today* **1997**, 36, 375-391.
- ⁷⁹ M. J. Girgis and B. C. Gates. Reactivities, reaction networks, and kinetics in high-pressure catalytic hydroprocessing. *Industrial & Engineering Chemistry Research* **1991**, 30, 2021-2058.
- ⁸⁰ H. Schulz, W. Böhringer, P. Waller and F. Ousmanov. Gas oil deep Hydrodesulfurization: refractory compounds and retarded kinetics. *Catalysis Today* **1999**, 49(1-3), 87-97.

APPENDIX A GC PARAMETER

Table A.1 HP5890 II GC Settings for ODS Product Analysis

Parameter	Setting
Injector Temperature	220 °C
Detector Temperature	220 °C
Initial Temperature	60°C
Initial Time	1 min
Ramp Rate	3 °C/min
Level 1 Temperature	69°C
Level 1 Ramp Rate	5°C
Level 1 Final Time	0 min
Level 2 Temperature	165°C
Level 2 Ramp Rate	15°C/min
Level 2 Final time	0 min
Final Temp	210°C
Final Time	5 min
Volumetric Flow through Column	2.6 mL/min
Split Vent Rate	70 mL/min
Auxiliary flow	20 mL/min
H ₂ flow	34 mL/min
Air flow	350 mL/min
Column	Econo-Cap EC1 Capillary Columns 30m * 0.32 mm (Alltech)

GC calibration:

A series of calibration sample was made by adding the fixed amount of internal standard (mesitylene) to the feed solution in which the composition are already known. And then each sample was analyzed by HP 5890 GC three times. The f_i calibration factor of compound i can be computed through Eq. A.1

$$f_i = \frac{A_i/A_s}{C_i/C_s} \text{ Eq.A.1}$$

In Eq.A.1, A_i is the peak area of compound i while A_s is the peak area of internal standard s . C_i is the molar concentration of compound i and C_s is the molar concentration of internal standard s .

Table A.2 Retention Times and Calibration Slopes of Feed Components

Compound	Retention Time (min)	Calibration Slope
Thiophene	1.75	2.01
Ethylbenzene	3.25	1.08
Mesitylene	5.13	1
1-methylnaphthalene	14.3	0.809
Hexadecane	23.1	0.513
Dibenzothiophene	24.6	0.715
Acridine	25.1	0.728
Carbazole	25.5	0.754

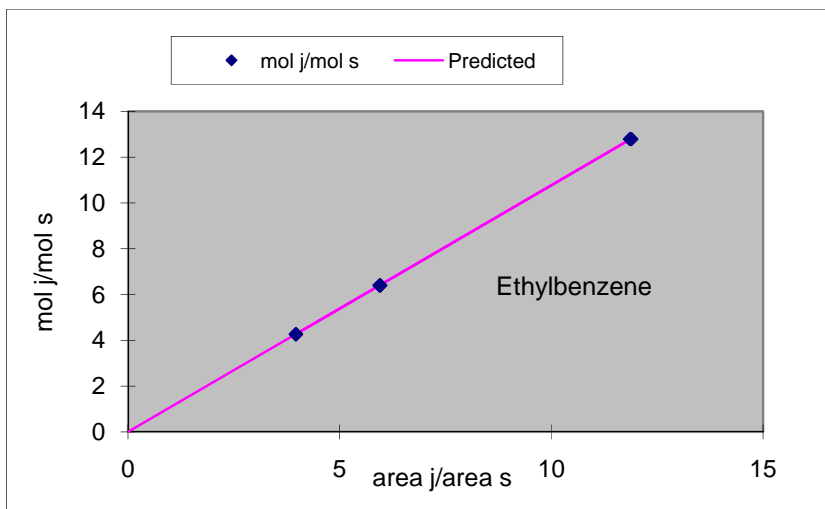


Figure A.1 Calibration Curve for ethylbenzene

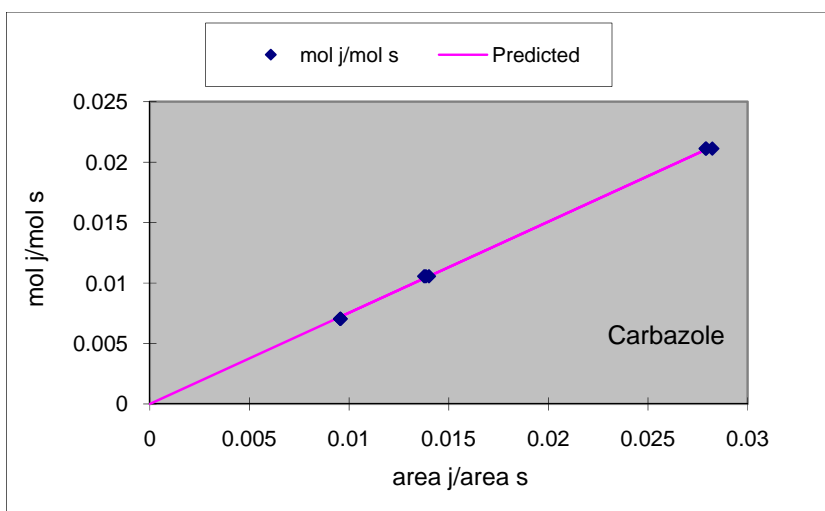


Figure A.2 Calibration Curve for carbazole

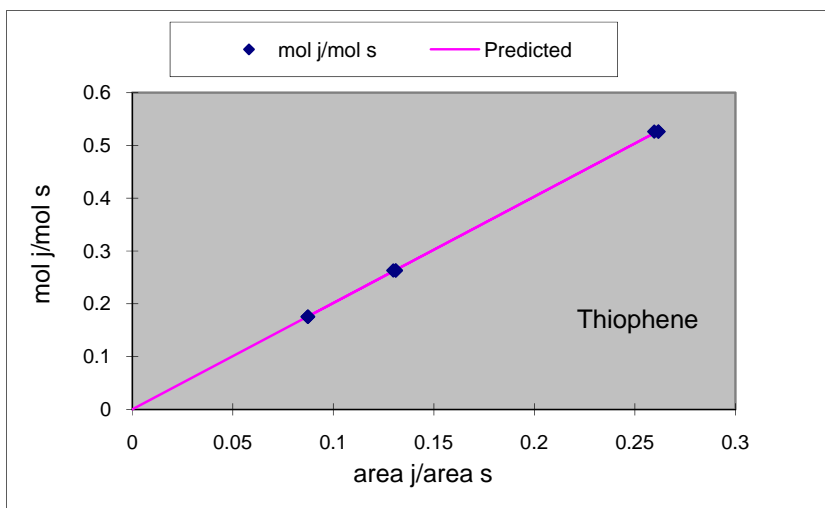


Figure A.3 Calibration Curve for thiophene

Table A.3 Composition of feed “F 7-28,2009”

Compound	Weight (g)	Wt %
Hexadecane	133.72	74.99
Ethylbenzene	21.41	12.01
1Methyl-Naphthalene	21.40	12.00
Carbazole	0.0557	0.03
Acridine	0.0362	0.02
Thiophene	0.6980	0.39
Dibenzothiophene	0.9831	0.55

Table A.4 Signal integration parameter

Integration Parameter	Value
Initial Area Reject	0
Initial Peak Width	0.05
Shoulder Detection	On
Initial Threshold	11.0
Area Reject	15000

APPENDIX B PROCEDURE TO PERFORM THE EXPERIMENT

B. 1 Procedure to Run the ODS test reactions - rocker reactor:

1. Load catalyst. If reduction is required, use procedure B.2 or B.3 as appropriate before proceeding.
2. Load 10 mL of feed mixture into the reactor under positive pressure of N₂, close valve.
3. Connect tubing to reactor, test for leaks, insulate.
4. Flush tubing with 0.45 MPa O₂ twice.
5. Set controller to desired temperature and set the pressure regulator of the O₂ cylinder to the desired pressure.
6. When the desired temperature is reached, open the valves and start the rocker. If the reaction conditions require closed valves, close the valves after 1 min.
7. When the reaction is finished, stop the rocker first, set the temperature controller to below RT, and close the cylinder valve.
8. Slowly open the system exhaust valve . After the pressure reaches atmospheric, close the reactor valves.
9. Disassemble the reactors.
10. Measure the total volume of liquid.
11. Take 2 vials of 4 mL product samples from each reactor. Before OD25, only one vial of product was collected from each reactor.
12. Remove the catalyst from the reactor and save.

B.2 Pretreatment of (some) catalysts under 40 vol% H₂/ 60 vol % N₂

1. Load and flush reactor with N₂, twice.
2. Fill reactor with 40 vol% H₂/N₂ to ~0.31 MPa.
3. Raise T to ~403 K, hold 4 h.
4. Cool to RT.

5. Isolate reactors, flush lines with N₂.
6. Fill reactors with 0.58 MPa N₂ and flush, twice, the last time leaving a slight positive pressure.

B. 3 Pretreatment of (some) catalysts with 20 vol% CH₄/80 vol % H₂

1. Fill reactor with 0.58 MPa N₂ and vent 3 times.
2. Shut valve to reactor.
3. Disconnect O₂/N₂ and connect CH₄/H₂.
4. Open the CH₄/H₂ cylinder and set the pressure regulator to 0.58 MPa
5. Open valve, fill with CH₄/H₂ and vent 3 times.
6. After the third fill, bring T to 403K, hold for 1 h.
7. Cool under CH₄/H₂.
8. Close valve to reactor and release the pressure.
9. Disconnect CH₄/H₂ line and connect to N₂ and O₂ lines.
10. Fill with N₂ and vent 3 times, the last time leaving a slight positive pressure.

APPENDIX C RAW DATA AND REACTION CONDITIONS

C. 1 Calculation for Conversions of each Compounds in ODS reaction.

Mesitylene was used as an internal standard. Before GC analyses, 40 μ L mesitylene was added to the 4 mL product samples.

From the GC results, the ratios of areas between peak *i* (reactant) and peak *s* (internal standard) were obtained. Then the conversion of each reactant compound was calculated as:

$$x_i = \left(\frac{C_i^o}{C_s^o} - f_i \times \frac{A_i}{A_s} \right) / \frac{C_i^o}{C_s^o} \quad \text{Equation C.1}$$

In Equation C.1, A_i is the peak area of reactant, A_s is the peak area of internal standard, C_i is the molar concentration of *i*, C_s is the molar concentration of internal standard, and f_i is the calibration factor (mol/area) of compound *i*.

Table C.1 Reactant conversions in ODS experiments

	OD13-1	OD15-1	OD16-1	OD18n-1	OD19-1	OD20-1	OD21-1	OD22n-1
Ethylbenzene	3.06%	4.36%	5.47%	5.52%	6.01%	10.26%	6.31%	9.84%
1-methylnaphthalene	3.78%	5.38%	6.22%	6.53%	6.24%	10.73%	6.59%	11.08%
Carbazole	11.89%	12.29%	21.86%	16.38%	15.60%	31.05%	14.25%	20.01%
Acridine	9.33%	9.33%	10.30%	17.89%	21.77%	13.13%	13.00%	27.29%
Thiophene	12.19%	12.81%	14.17%	13.72%	13.62%	16.92%	16.11%	16.59%
DBT	8.73%	9.00%	10.55%	11.31%	12.23%	14.04%	11.37%	15.80%
	OD13-2	OD15-2	OD16-2	OD18n-2	OD19-2	OD20-2	OD21-2	OD22n-2
Ethylbenzene	3.64%	5.15%	5.10%	5.05%	8.01%	10.90%	5.70%	10.32%
1-methylnaphthalene	1.83%	3.66%	4.94%	5.13%	4.60%	9.50%	6.57%	9.73%
Carbazole	7.18%	9.76%	12.41%	12.89%	15.87%	29.83%	15.43%	16.35%
Acridine	4.40%	4.24%	8.59%	14.43%	17.77%	11.14%	13.72%	24.58%
Thiophene	15.73%	15.46%	15.78%	12.78%	25.31%	20.45%	16.28%	18.38%
DBT	6.31%	6.95%	8.99%	10.31%	11.42%	13.29%	11.78%	13.87%

	OD23-1	OD24n-1	OD25-1	OD26-1	OD27-1	OD28-1	OD29-1	OD30-1
Ethylbenzene	6.13%	9.63%	-0.22%	1.85%	1.52%	2.84%	0.07%	2.69%
1-methylnaphthalene	6.93%	9.29%	-0.53%	2.34%	2.81%	1.27%	-0.76%	0.64%
Carbazole	21.42%	26.68%	-6.49%	15.84%	16.78%	23.73%	0.41%	10.85%
Acridine	26.75%	12.59%	0.47%	23.18%	24.74%	2.02%	15.31%	30.71%
Thiophene	14.27%	21.98%	3.59%	6.67%	6.69%	11.50%	6.52%	8.43%
DBT	15.32%	13.13%	-2.15%	4.50%	6.29%	-0.30%	2.64%	9.85%

Table C.1 Continue

	OD23-2	OD24n-22	OD 25-2	OD26-2	OD27-2	OD28-2	OD29-2	OD30-2
Ethylbenzene	5.62%	9.35%	0.51%	2.53%	3.06%	2.53%	0.93%	2.99%
1-methylnaphthalene	6.87%	7.46%	-0.45%	0.56%	-0.54%	0.56%	-3.33%	-1.79%
Carbazole	21.57%	22.61%	-5.13%	11.19%	8.28%	23.38%	-4.43%	3.08%
Acridine	26.94%	8.88%	1.57%	18.74%	17.11%	1.25%	9.13%	24.88%
Thiophene	13.72%	22.62%	5.73%	8.49%	9.96%	11.01%	8.72%	9.37%
DBT	16.66%	11.07%	-0.65%	2.76%	1.57%	0.85%	-1.44%	5.90%

	OD31-1	OD32-1	OD32-n1	OD33-1	OD34-1	OD35 -1	OD35n-1	OD36-1
Ethylbenzene	3.90%	-2.85%	3.98%	0.15%	0.84%	1.26%	2.33%	1.69%
1-methylnaphthalene	0.09%	-5.07%	3.88%	-0.37%	-0.09%	0.41%	1.65%	0.46%
Carbazole	11.08%	9.87%	21.68%	15.24%	5.39%	-2.69%	-0.92%	3.40%
Acridine	-1.27%	15.62%	26.06%	39.07%	36.27%	0.99%	1.77%	8.53%
Thiophene	11.14%	4.96%	13.46%	3.21%	4.25%	2.85%	6.68%	5.65%
DBT	-2.06%	-1.79%	9.28%	-1.33%	0.94%	-0.16%	0.88%	1.25%
	OD31-2	OD32-2	OD32-n2	OD33-2	OD34-2	OD35-2	OD35n-2	OD36-2
Ethylbenzene	3.29%	-2.98%	3.44%	0.50%	0.86%	3.48%	2.32%	1.84%
1-methylnaphthalene	0.23%	-4.51%	2.82%	-0.46%	-0.19%	-1.80%	0.82%	-0.01%
Carbazole	13.15%	11.32%	19.43%	14.03%	5.26%	-10.37%	-3.72%	-0.61%
Acridine	0.09%	16.93%	23.32%	38.56%	35.72%	-7.18%	-0.75%	6.20%
Thiophene	10.17%	5.00%	12.90%	4.10%	4.27%	8.95%	6.10%	5.59%
DBT	-1.05%	-0.76%	7.05%	-1.98%	0.61%	-8.25%	-1.60%	-0.26%

	OD37-1	OD38-1	OD39-1	OD40-1	OD41-1	OD42-1	OD43-1	OD44-1
Ethylbenzene	25.29%	-1.91%	-2.51%	-0.21%	-1.98%	0.08%	1.74%	-0.49%
1-methylnaphthalene	-2.63%	-1.36%	-0.68%	-1.37%	-0.20%	-1.97%	0.62%	-2.19%
Carbazole	-7.92%	-0.25%	-1.64%	-2.92%	3.03%	3.47%	-3.18%	27.35%
Acridine	0.00%	9.18%	20.33%	0.13%	7.60%	15.60%	-2.98%	-3.08%
Thiophene	72.16%	3.18%	3.13%	5.13%	1.02%	4.18%	4.82%	4.06%
DBT	-1.03%	-1.31%	-0.33%	-2.73%	0.22%	-3.52%	-1.43%	-3.98%
	OD37-2	OD38-2	OD39-2	OD40-2	OD41-2	OD42-2	OD43-2	OD44-2
Ethylbenzene	25.45%	-2.33%	-2.51%	-0.26%	-1.81%	0.03%	1.84%	-0.55%
1-methylnaphthalene	-2.19%	-0.84%	-0.72%	-1.02%	-0.58%	-2.04%	0.62%	-1.90%
Carbazole	-14.71%	0.73%	-1.87%	-1.48%	3.73%	3.72%	-3.25%	29.23%
Acridine	-1.03%	10.39%	20.31%	1.13%	7.10%	15.58%	-2.72%	-2.50%
Thiophene	71.94%	1.96%	3.16%	4.63%	1.36%	4.14%	5.13%	3.95%
DBT	-1.86%	0.18%	-0.46%	-2.00%	-0.37%	-3.72%	-1.25%	-3.42%

	OD45-1	OD46-1	OD47-1	OD48-1	OD49-1	OD50-1	OD51-1	OD52-1
Ethylbenzene	1.35%	-1.40%	0.15%	0.77%	-0.32%	0.53%	0.89%	0.62%
1-methylnaphthalene	2.55%	0.27%	2.00%	2.30%	-1.21%	-1.03%	-1.52%	-2.81%
Carbazole	4.38%	29.67%	21.63%	24.63%	-0.92%	23.39%	6.46%	-3.43%
Acridine	3.90%	31.62%	26.36%	4.85%	2.41%	28.97%	21.42%	0.41%
Thiophene	4.47%	7.96%	4.95%	3.93%	6.55%	12.39%	10.69%	7.76%

Table C.1 Continue

DBT	2.27%	4.18%	6.57%	2.29%	-1.08%	1.99%	-1.79%	-3.68%
	OD45-2	OD46-2	OD47-2	OD48-2	OD49-2	OD50-2	OD51-2	OD52-2
Ethylbenzene	1.18%	-1.36%	-0.18%	1.59%	-0.48%	0.71%	0.94%	0.68%
1-methylnaphthalene	2.42%	-0.18%	1.53%	-1.50%	-0.76%	-1.49%	-1.97%	-3.09%
Carbazole	3.77%	27.77%	20.81%	14.67%	-1.53%	21.84%	7.14%	-2.98%
Acridine	6.04%	29.75%	26.09%	-4.98%	1.22%	28.18%	21.55%	0.49%
Thiophene	4.23%	5.38%	4.86%	6.73%	6.23%	12.85%	10.55%	7.90%
DBT	2.28%	1.97%	6.24%	-4.03%	-1.35%	1.00%	-1.69%	-3.86%

	OD53-1	OD54-1	OD55-1	OD56-1	OD57-1	OD58-1	OD59-1	OD60-1
Ethylbenzene	-0.85%	-0.56%	4.30%	0.31%	1.61%	0.84%	2.12%	17.65%
1-methylnaphthalene	-2.13%	2.67%	3.79%	-0.48%	2.90%	0.41%	1.95%	-0.42%
Carbazole	-2.53%	34.75%	21.37%	7.92%	26.50%	4.53%	2.75%	-5.99%
Acridine	-2.00%	35.93%	25.30%	32.96%	31.55%	6.49%	22.19%	26.24%
Thiophene	3.35%	6.76%	9.79%	5.17%	14.34%	8.29%	9.99%	64.66%
DBT	-1.55%	10.24%	7.08%	7.96%	8.59%	1.89%	7.19%	-0.72%
	OD53-2	OD54-2	OD55-2	OD56-2	OD57-2	OD58-2	OD59-2	OD60-2
Ethylbenzene	-0.92%	-1.04%	4.12%	0.20%	1.58%	0.83%	2.03%	17.90%
1-methylnaphthalene	-2.28%	2.89%	3.59%	0.05%	2.85%	0.78%	1.87%	-0.26%
Carbazole	-4.28%	35.96%	19.21%	10.48%	27.79%	3.99%	2.41%	-6.08%
Acridine	-1.75%	38.15%	24.53%	34.03%	31.65%	6.03%	21.31%	26.58%
Thiophene	2.68%	4.68%	8.86%	5.15%	14.59%	8.44%	9.80%	64.83%
DBT	-1.63%	11.44%	6.70%	8.86%	8.61%	1.52%	6.82%	-0.52%

	OD61-1	OD62-1	OD63-1	OD64-1	OD65-1	OD66-1	OD67-1	OD68-1
Ethylbenzene	5.71%	7.03%	9.88%	5.46%	3.46%	4.02%	3.10%	4.68%
1-methylnaphthalene	6.49%	7.06%	8.78%	4.62%	2.19%	2.14%	2.01%	5.40%
Carbazole	29.56%	27.58%	14.23%	10.15%	3.94%	7.22%	6.20%	28.90%
Acridine	31.47%	29.90%	28.05%	32.42%	7.30%	9.13%	9.70%	52.48%
Thiophene	16.86%	18.56%	18.32%	14.58%	13.06%	15.80%	12.84%	14.25%
DBT	12.82%	12.02%	12.37%	6.11%	4.20%	3.68%	4.62%	13.29%
	OD61-2	OD62-2	OD63-2	OD64-2	OD65-2	OD66-2	OD67-2	OD68-2
Ethylbenzene	6.27%	7.31%	9.62%	5.74%	3.62%	3.88%	3.26%	4.72%
1-methylnaphthalene	6.30%	7.27%	9.10%	4.83%	2.07%	2.21%	1.85%	5.28%
Carbazole	29.03%	27.92%	14.34%	9.80%	4.51%	6.85%	5.96%	29.15%
Acridine	31.46%	30.22%	28.31%	32.23%	6.75%	9.32%	9.20%	51.86%
Thiophene	17.92%	18.96%	17.93%	15.08%	13.54%	15.43%	13.35%	14.74%
DBT	12.63%	12.40%	12.73%	6.19%	3.85%	3.87%	4.35%	12.92%

	OD69-1	OD70-1	OD71-1	OD72-1	OD73-1	OD74-1	OD75-1	OD76-1
Ethylbenzene	10.49%	5.80%	6.87%	9.60%	5.56%	7.88%	8.11%	7.45%
1-methylnaphthalene	9.74%	4.87%	5.90%	7.57%	3.45%	5.13%	5.32%	4.25%
Carbazole	17.76%	39.28%	27.79%	41.46%	18.28%	9.27%	12.84%	6.48%
Acridine	21.76%	44.11%	42.32%	66.52%	27.12%	12.93%	21.97%	9.23%
Thiophene	21.18%	22.26%	19.59%	25.13%	20.63%	22.12%	23.24%	20.91%
DBT	11.64%	12.95%	16.20%	18.47%	11.64%	7.49%	6.79%	6.24%

Table C.1 Continue

	OD69-2	OD70-2	OD71-2	OD72-2	OD73-2	OD74-2	OD75-2	OD76-2
Ethylbenzene	10.59%	5.68%	6.90%	9.68%	5.88%	8.20%	8.11%	7.43%
1-methylnaphthalene	9.85%	4.96%	5.85%	7.51%	3.23%	4.95%	5.46%	4.05%
Carbazole	17.17%	38.90%	26.94%	40.65%	18.47%	8.22%	13.85%	5.50%
Acridine	21.01%	44.32%	42.20%	66.08%	27.22%	11.61%	22.83%	8.40%
Thiophene	21.50%	21.84%	19.70%	25.40%	21.38%	22.94%	23.17%	20.80%
DBT	12.03%	13.37%	16.17%	17.65%	11.97%	6.27%	7.96%	5.21%

C. 2 Reaction Conditions:

The reaction conditions and catalysts used in these reactions are recorded in Table C.2.

They are categorized by groups of 4, because 4 reactors were used simultaneously.

Table C.2 Reaction conditions in Each ODS experiment

OD 1- OD4	T = 323K; Time = 3 h; no catalyst; Feed: 10 mL old feed
OD-1	P = 0.170 MPa
OD-2	P = 0.308 MPa
OD-3	P = 0.446 MPa
OD-4	P = 0.584 MPa
OD 5- OD8	T = 323K; P = 0.446 MPa; Time = 3 h; Feed: 10 mL old feed
OD-5	Catalyst = AL-3945E(Crushed) (0.2003g)
OD-6	Catalyst = V-275 1.2SW/AL-MPI H ⁺ (0.2010g)
OD-7	Catalyst = ZC-1 (0.1997g)
OD-8	Catalyst = Calcined Zeolyst MFI (0.2007g)
Date	2/23/2009
OD 9- OD 12:	T = 313K; Time = 1 h; Feed: 10 mL old feed
OD-9	Catalyst = ZC-1 (0.1007g); P = 0.173 MPa
OD-10	Catalyst = ZC-1 (0.1001g); P = 0.446 MPa
OD-11	P = 0.173 MPa; No catalyst
OD-12	P = 0.446 MPa; No catalyst
Date	3/20/2009
OD 13- OD 16	T= 323K; P=0.446 MPa; Time = 1 h; Feed: 10 mL old feed
OD-13	Catalyst = ReSi1(0.1014g)
OD-14	Catalyst = CsHPW/SiO ₂ (0.1015g)
OD-15	Catalyst = 7.9% CuO/TiO ₂ (0.1005g)
OD-16	Catalyst = CoSi1 (0.1003g)
Date	4/17/2009

Table C.2 Continue

OD 17- OD 20	T=343K; P=0.584 MPa; Time= 2 h; Feed: 10 mL old feed
OD-17	Catalyst = 7.9% CuO/TiO ₂ (0.1010g)
OD-18	Catalyst = CsHPW/SiO ₂ (0.0998g)
OD-19	Catalyst = ReSi1(0.1007g)
OD-20	Catalyst = CoSi1 (0.0998g)
Date	5/21/2009
Pretreatm ent of catalyst:	Cobalt catalyst dried at 373K in vaccum; others dried at 573K in air.

OD 21- OD 24	T=343K; P=0.446 MPa; Time = 2 h, Feed: 10 mL old feed
OD-21	Catalyst = 7.9% CuO/TiO ₂ (0.1004g)
OD-22	Catalyst = CsHPW/SiO ₂ (0.0994g)
OD-23	Catalyst = ReSi1(0.1001g)
OD-24	Catalyst = CoSi1 (0.1000g)
Date	5/28/2009
Pretreatm ent of catalyst:	Cobalt catalyst dried at 373K in vaccum; others dried at 573K in air.

OD 25- OD 28	T=343K; P= 0.584 MPa; Time = 2 h; Valve =open; Feed: 10 mL F 6-4, 2009
OD-25	Catalyst = 5%Pd/BaSO ₄ (0.1001g)
OD-26	Catalyst = 5%Pd/C Engelhard (0.1001g)
OD-27	Catalyst = 5%Pd/MPT-5 (0.1006g)
OD-28	Catalyst = CoSi1 (0.0997g)
Date	6/24/2009
Pretreatm ent of catalyst:	All catalysts were under 4 h reduction at 403K in 40 vol% H ₂ /N ₂ .

OD 29- OD 32	T=363K; P=0.791 MPa; Time= 2 h; Feed: 10 mL F 6-4, 2009
OD-29	Catalyst = CsHPW/SiO ₂ (0.1001g)
OD-30	Catalyst = ReSi1(0.1003g)
OD-31	Catalyst = CoSi1 (0.1004g)
OD-32	Catalyst = 5%Pd/MPT-5 (0.1006g)
Date:	7/1/2009
Pretreatm ent of catalyst:	All catalysts were under 4 h reduction at 403K in 40% H ₂ /N ₂ , OD 29 and OD 30 were dried at 573K for 2 h in air first.

OD 33- od36	T=363K; P=0.791 MPa; Time= 2 h; Feed: 10 mL F 7-10, 2009
OD-33	Catalyst = Cs _{2.5} H _{0.5} PW ₁₂ , exxon 21583-7-1 (0.3002g)
OD-34	Catalyst = (NH ₄) ₃ H ₂ PMo ₁₂ (0.3006g)
OD-35	Catalyst = (NH ₄) ₅ H ₄ PV ₆ W ₆ (0.3008g)
OD-36	Catalyst = Cs _{2.5} Ni _{0.08} H _{0.34} PMo ₁₂ (0.3012g)
Date:	7/10/2009

Table C.2 Continue

Pretreatment of catalyst:	None
OD 37-40	T=363K; P=0.791 MPa; Time= 2 h; Feed: 10 mL F 7-10, 2009
OD-37	Blank (No catalys)
OD-38	Catalyst = ZC-1 (0.0990g)
OD-39	Catalyst = V-275/MPI H+ (0.0993g)
OD-40	Catalyst = AL-3945E (0.1020g)
Date:	7/28,2009
Pretreatment of catalyst:	None
OD 41-44	T=343K; P=0.584 MPa; Time = 2 h; Feed: 10 mL F 7-10,2009
OD-41	Catalyst = 7.9% CuO/TiO ₂ (0.0997g)
OD-42	Catalyst = CsHPW/SiO ₂ (0.1003g)
OD-43	Blank
OD-44	Catalyst = CoSi1 (0.0998g)
Date:	8/3,2009
Pretreatment of catalyst:	CoSi1 dried at 373K for 1 h under vaccum; other two dried at 573K in air for 3 h.
OD 45-OD 48	T=343K; P=0.584 MPa; Time= 2 h; Feed: 10 mL F 7-10,2009
OD-45	Blank
OD-46	Catalyst = 5% Pd/C Engelhard (0.1033g)
OD-47	Catalyst = 5% Pd/MPT-5 (0.1018g)
OD-48	CoSi1 (0.1008g)
Date:	8-5,2009
Pretreatment of catalyst:	All the three catalysts were under reduction in reactor at 403K in atmosphere of 0.584 MPa of 20 vol%CH ₄ /H ₂ for 1h.
OD 49-OD 52	T=363K; P=0.791 MPa; Time= 3 h; Feed: 10 mL F 7-10, 2009
OD-49	Blank
OD-50	Catalyst = 5% Pd/C Engelhard (0.1003g)
OD-51	Catalyst = 5% Pd/Degussa E5 (0.1012g)
OD-52	Catalyst = 0.5% Pd/Al ₂ O ₃ (Sasol HTA-101 gamma alumina) (0.1002g)
Date	8-17, 2009
Pretreatment of catalyst:	All the three catalysts were under 1h reduction at 403K within 20 vol%CH ₄ /80 vol%H ₂ atmosphere, then flushing within N ₂ prior to reaction.
OD 53-OD 56	T= 343K; P=0.791 MPa; Time = 4 h; Feed: 10 mL F 7-10,2009
OD-53	Blank
OD-54	Catalyst = 5% Pd/C MPT-5 (0.1017g)
OD-55	Catalyst = 5% Pd/Degussa E5 (0.1009g)

Table C.2 Continue

OD-56	Catalyst = ReSi1(0.1022g)
Date	9-1,2009
Pretreatment of catalyst:	All the three catalysts were under 1 h reduction at 493K within 20 vol%CH ₄ /80 vol%H ₂ atmosphere, then flushed with N ₂ prior to reaction.
OD 57 - OD 60	T= 363K; P=0.791 MPa; Time = 4 h; Feed: 10 mL F 7-10,2009
OD-57	Catalyst = 5% Pd/C MPT-5 (0.1003g)
OD-58	Catalyst = 0.5% Pt/Al ₂ O ₃ (aldrich) (0.1017g)
OD-59	Catalyst = ReSi1(0.1003g)
OD-60	Catalyst = CDX6 (0.1017g)
Date	9-9,2009
Pretreatment of catalyst:	All the catalysts were under 1 h reduction at 493K within 40 vol% H ₂ /N ₂ atmosphere, then flushed with N ₂ prior to reaction.
OD 61- OD 64	T= 343K; P=1.825 MPa; Time = 4 h; Feed: 10 mL F 7-28,2009
OD-61	Catalyst = 5% Pd/MPT-5 (0.1001g)
OD-62	Catalyst = 5% Pd/Degussa E-5 (0.1039g)
OD-63	Catalyst = ReSi1(0.1005g)
OD-64	Catalyst = CDX6 (0.1014g)
Date	9-17, 2009
Pretreatment of catalyst:	The 5%Pd/Degussa E5 was dried in air at 473K overnight. After that all the catalysts were under 2 h reduction at 493K within 40% H ₂ /N ₂ atmosphere, then flushed with N ₂ prior to reaction.
OD 65- OD 68	T =343K; P=1.825 MPa; Time= 4 h; Feed: 10 mL F 7-28,09
OD-65	blank
OD-66	Catalyst = CDX5(3) (0.1007g)
OD-67	Catalyst = CDX4 (0.0997g)
OD-68	Catalyst = CDX3 (0.1004g)
Date	9/25,2009
Pretreatment of catalyst:	1 h reduction in 40 vol% H ₂ /60 vol% N ₂ at 448K.
OD 69-72	T=343K;P=1.136 MPa; Time= 4 h; Feed: 10 mL F 7-28,09
OD-69	Catalyst = CDX5(3) (0.1024g)
OD-70	Catalyst = 5%Pd/MPT-5 (0.1012g)
OD-71	Catalyst = CDX3 (0.1004g)
OD-72	Catalyst = CDX2 (0.1009g)
Date	9/30,2009
Pretreatment of catalyst:	1 h reduction in 40 vol% H ₂ /60 vol% N ₂ at 448K.
OD 73-76	T=343K; P= 0.791 MPa; Time = 4 h; Feed: 10 mL F 7-28,09
OD-73	Catalyst = CDX3 (0.1027g)
OD-74	Catalyst = CDX4 (0.1043g)

Table C.2 Continue

OD-75	Catalyst = Pt-S2 (0.1034g)
OD-76	Catalyst = 1%Pt/Zn/K/Al ₂ O ₃ (0.1066g)
Date	2-4, 2010
Pretreatment of catalyst:	1h reduction in 20 vol%CH ₄ /80 vol%H ₂ at 448K and at 0.308MPa.

C.3 Feed Compositions:

Table C.4 Compositions in feed “F 7-10, 2009”

Compound	Weight (g)	Wt %
Hexadecane	225.0	75.00
Ethylbenzene	35.9971	12.00
1methyl-naphthalene	35.9858	12.00
Carbazole	0.0903	0.03
Acridine	0.0608	0.02
Thiophene	1.2056	0.40
Dibenzothiophene	1.6517	0.55

Table C.5 Compositions in feed “F 7-28, 2009”

Compound	Weight (g)	Wt %
Hexadecane	133.72	74.99
Ethylbenzene	21.4140	12.01
1methyl-naphthalene	21.3991	12.00
Carbazole	0.0557	0.03
Acridine	0.0362	0.02
Thiophene	0.6980	0.39
Dibenzothiophene	0.9831	0.55

Table C.6 Compositions in feed “F 6-4, 2009”

Compound	Weight (g)	Wt %
Hexadecane	112.5	74.98
Ethylbenzene	18.0300	12.02
1methyl-naphthalene	18.0040	12.00
Carbazole	0.0453	0.03
Acridine	0.0313	0.02
Thiophene	0.6003	0.40
Dibenzothiophene	0.8230	0.55

APPENDIX D CATALYST CHARACTERIZATION

D.1 Elemental Analysis

Elemental analysis was performed using inductively coupled plasma atomic emission spectroscopy (ICP-AES). A known amount of catalyst sample was dissolved in boiling nitric acid under reflux for three times, and then diluted with DI water. The ICP concentrations of the calibration samples are shown in Table D.1. The loadings of catalysts are shown in Table D.2.

Table D.1 ICP calibration

Sample Name	Expected Conc.	Pd 229	Pd 324	Pd 340	Pd 360	Average
PPM						
Std1	0	0.01	0.089	0.009	0.0076	0.0289
Std2	1	0.977	0.991	0.977	0.966	0.977
Std3	5	4.949	4.829	4.825	4.864	4.866
Check Std	30	29.64	29.36	29.10	29.27	29.34

Table D.2 Catalyst Loadings by ICP-AES

Sample Name	ICP measurement (PPM)	Catalyst (g)	Catalyst loading wt%
CDX7-ICP1	405.20	1.0560	3.84
CDX7-ICP2	272.96	0.6989	3.91
CDX8-ICP1	310.68	1.0100	3.08
CDX8-ICP2	119.44	0.9724	1.24

D.2 Dispersion Measurements

All Pd dispersions were measured using a Micromeritics Pulsesorb 2700 instrument. A fixed volume of analysis gas (H_2) is introduced into a sample tube which is under a constant flow of N_2 gas. The Pulsesorb detects the amount of gas that does not adsorb on the catalyst sample by a thermal conductivity detector. The N_2 and H_2 gas phases must have significantly different thermal conductivities. Results from a typical experiment are shown in Table D.3.

Table D.3 Chemisorption experiment (0.5 wt% Pt on Al₂O₃) using H₂.

Inject ion #	Loop Volume (cm ₃)	TCD Area
1	0.0891	0.00
2	0.0891	0.06
3	0.0891	0.40
4	0.0891	0.49
5	0.0891	0.50
6	0.0891	0.50
7	0.0891	0.50

The calibration constant (*k*) value for this run is 0.0891/0.50, or 0.1782 cm³. The total volume of gas chemisorbed is:

$$\text{1st injection: } 0.0891 - 0 = 0.0891$$

$$\text{2nd injection: } 0.0891 - (0.06 \times 0.1782) = 0.0784$$

$$\text{3rd injection: } 0.0891 - (0.40 \times 0.1782) = 0.0178$$

$$\text{4th injection: } 0.0891 - (0.49 \times 0.1782) = 0.0018$$

$$\text{Total volume: } 0.1871 \text{ cm}^3$$

The volume is brought to STP using the ideal gas law. The percent dispersion *D* is calculated as:

$$D = \frac{V_{ads} M S}{W V_m f} \cdot 100$$

where V_{ads} is the total volume adsorbed at STP, M is the molecular weight of the catalytic metal, S the adsorption stoichiometry (in mol active metal/mol test gas), W the weight of catalyst sample, V_m the molar volume at STP (22414 cm³/mol), and f the weight fraction of catalyst metal on the support. All of these parameters are well known except S . There is some uncertainty in how different types of adsorbates bond to active metals on a

surface. It is generally accepted that one molecule of H₂ will dissociate and occupy two active metal sites, S = 0.5.

Table D.4 Chemisorption experiment (5 wt% Pd on Degussa E5) using H₂.

Injection #	Loop Volume (cm ₃)	TCD Area
1	0.097	0.07
2	0.097	0.09
3	0.097	0.12
4	0.097	0.16
5	0.097	0.18
6	0.097	0.20
7	0.097	0.20
8	0.097	0.20
9	0.097	0.20
10	0.097	0.21
11	0.097	0.21
12	0.097	0.21
13	0.097	0.21

Pretreatment: N₂ flow (50 mL/min) during temperature ramp to 493K, and then hold for 30 min. Cool with water.

Catalyst weight: 0.0324g

Dispersion: 29.029%

Table D.5 Chemisorption experiment (CDX7) using H₂.

Injection #	Loop Volume (cm ₃)	TCD Area
1	0.097	0
2	0.097	0.03
3	0.097	0.03
4	0.097	0.04
5	0.097	0.05
6	0.097	0.05
7	0.097	0.06
8	0.097	0.08
9	0.097	0.08
10	0.097	0.09
11	0.097	0.10

Table D.5 Continue

12	0.097	0.12
13	0.097	0.11
14	0.097	0.11
15	0.097	0.11
16	0.097	0.11
17	0.097	0.11
18	0.097	0.13
19	0.097	0.13
20	0.097	0.13
21	0.097	0.13
22	0.097	0.13
23	0.097	0.13
24	0.097	0.13
25	0.097	0.13
26	0.097	0.14
27	0.097	0.145
28	0.097	0.16
29	0.097	0.145
30	0.097	0.16
31	0.097	0.17
32	0.097	0.18
33	0.097	0.18
34	0.097	0.18
35	0.097	0.19
36	0.097	0.19
37	0.097	0.19
38	0.097	0.19
39	0.097	0.19

Pretreatment: Clean for 1.5 h in 20 vol% H_2/N_2 at 523K. Then switch to 50 mL/min N_2 and hold at 523K for 20 min. Cool with water.

Catalyst weight: 0.098g

Dispersion: 78.77%

Table D.6 Chemisorption experiment (CDX8) using H_2 .

Injection #	Loop Volume (cm ₃)	TCD Area
1	0.097	0
2	0.097	0
3	0.097	0.03
4	0.097	0.13
5	0.097	0.16

Table D.6 Continue

6	0.097	0.16
7	0.097	0.16
8	0.097	0.16
9	0.097	0.16
10	0.097	0.18
11	0.097	0.19
12	0.097	0.19
13	0.097	0.19
14	0.097	0.19
15	0.097	0.19
16	0.097	0.19
17	0.097	0.19
18	0.097	0.19
19	0.097	0.19
20	0.097	0.19
21	0.097	0.19
22	0.097	0.20
23	0.097	0.20
24	0.097	0.20
25	0.097	0.20
26	0.097	0.20
27	0.097	0.20

Pretreatment: Clean for 1.5 h in 20 vol% H₂/N₂ at 523K. Then switch to 50 mL/min N₂ and hold at 523K for 20 min. Cool with water.

Catalyst weight: 0.1095g

Dispersion: 30.54%

Table D.7 cChemisorption experiment (CDX6) using H₂.

Injection #	Loop Volume (cm ₃)	TCD Area
1	0.097	0.03
2	0.097	0.17
3	0.097	0.21
4	0.097	0.22
5	0.097	0.23
6	0.097	0.23
7	0.097	0.23
8	0.097	0.21
9	0.097	0.23
10	0.097	0.23
11	0.097	0.23

Pretreatment: Sample treated in 48 mL/min N₂ during the temperature ramp to 773 K. Then switch to 60 mL/min air at 773 K for 4h, then 48 mL/min N₂ while lowering the temperature to 448 K. Switch to 60 mL/min H₂ and hold at 448 K for 1h. Switch to 48 mL/min N₂ flow, hold at 483 K for 20 min. Cool with water.

Catalyst weight: 0.0751g

Dispersion: 9.31%

Table D.8 Chemisorption experiment (CDX5) using H₂.

Injection #	Loop Volume (cm ₃)	TCD Area
1	0.097	0.14
2	0.097	0.04
3	0.097	0.03
4	0.097	0.04
5	0.097	0.06
6	0.097	0.10
7	0.097	0.12
8	0.097	0.13
9	0.097	0.18
10	0.097	0.20
11	0.097	0.21
12	0.097	0.21
13	0.097	0.22
14	0.097	0.22
15	0.097	0.22
16	0.097	0.22
17	0.097	0.22
18	0.097	0.22
19	0.097	0.22

Pretreatment: Sample treated in 50 mL/min 20% H₂ during the temperature ramp to 623 K, then held at 623K for 1 h. Switch to 50 mL/min N₂. Raise the temperature to 723K and hold for 30 min. Cool with water.

Catalyst weight: 0.0521g

Dispersion: 56.39%

VITA

Dongxing Liu was born to Jianming Liu and Guoqin Li in the month of November, 1983, in Jixian, Tianjin, a port city just east of Beijing, China. He completed his undergraduate studies at the Tianjin University, where he earned the degree of Bachelor of Science in Chemical Engineering in 2007. After that, he left his home country and enrolled at Louisiana State University in the Department of Chemical Engineering where he worked under the supervision of Dr. Kerry M. Dooley and Dr. F. Carl. Knopf. He looks forward to an industrial or government career in China.